

Prep1.1 has essential genetic functions in hindbrain development and cranial neural crest cell differentiation

Gianluca Deflorian¹, Natascia Tiso¹, Elisabetta Ferretti², Dirk Meyer³, Francesco Blasi², Marino Bortolussi¹ and Francesco Argenton^{1,*}

¹Dipartimento di Biologia, Università di Padova, Via U. Bassi 58/B, 35131 Padova, Italy

²Department of Molecular Biology and Functional Genomics, Università Vita Salute San Raffaele and San Raffaele Scientific Institute, Via Olgettina, 58, 20132 Milano, Italy

³Department of Developmental Biology, University of Freiburg, Hauptstrasse 1, D-79104 Freiburg, Germany

*Author for correspondence (e-mail: francesco.argenton@unipd.it)

Accepted 27 October 2003

Development 131, 613-627
Published by The Company of Biologists 2004
doi:10.1242/dev.00948

Summary

In this study we analysed the function of the Meinox gene *prep1.1* during zebrafish development. Meinox proteins form heterotrimeric complexes with Hox and Pbx members, increasing the DNA binding specificity of Hox proteins in vitro and in vivo. However, a role for a specific Meinox protein in the regulation of Hox activity in vivo has not been demonstrated. In situ hybridization showed that *prep1.1* is expressed maternally and ubiquitously up to 24 hours post-fertilization (hpf), and restricted to the head from 48 hpf onwards. Morpholino-induced *prep1.1* loss-of-function caused significant apoptosis in the CNS. Hindbrain segmentation and patterning was affected severely, as revealed by either loss or defective expression of several hindbrain markers (*foxb1.2/mariposa*, *krox20*, *pax2.1* and *pax6.1*), including anteriorly expressed Hox genes (*hoxb1a*, *hoxa2* and *hoxb2*), the impaired migration

of facial nerve motor neurons, and the lack of reticulospinal neurons (RSNs) except Mauthner cells. Furthermore, the heads of *prep1.1* morphants lacked all pharyngeal cartilages. This was not caused by the absence of neural crest cells or their impaired migration into the pharyngeal arches, as shown by expression of *dlx2* and *snail1*, but by the inability of these cells to differentiate into chondroblasts. Our results indicate that *prep1.1* has a unique genetic function in craniofacial chondrogenesis and, acting as a member of Meinox-Pbc-Hox trimers, it plays an essential role in hindbrain development.

Key words: Vertebrate, Zebrafish, Hox, Pbx, Meis, Prep, Rhombomere, Segmentation, Neural Crest, Pharyngeal arch, Morpholino

Introduction

Segmentation is an essential, evolutionarily conserved, step in embryonic development that allows the generation and determination of different parts of the body. The *Hox* genes are key players in segmental determination through their combined expression in individual segments (Krumlauf, 1994; Moens and Prince, 2002). Spatial-specific and temporal-specific gene expression is regulated by mechanisms generated by combinatorial interactions of individual transcription factors. The segmentation of the vertebrate hindbrain, for example, relies on the rhombomere-specific expression of a subset of *Hox* genes. *Hox* gene products, in turn, gain high specificity for DNA target sequences by interacting with Pbc (Pbx in vertebrates) members of the TALE family of homeodomain proteins (Burglin, 1997; Kamps et al., 1990; Nourse et al., 1990). Four *Pbx* genes have been identified in mammals and five in zebrafish (Mann and Chan, 1996; Moens and Prince, 2002; Waskiewicz et al., 2002).

A further subfamily of homeodomain transcription factors, which are also members of the TALE family, is involved in the Hox regulation machinery. These are the Meinox proteins (Burglin, 1997). In vertebrates, the Meinox subfamily include Meis and Prep proteins, whereas a single member occurs in

Drosophila (Hth) and *Caenorhabditis* (UNC-62) (Van Auken et al., 2002). The interaction between Meinox and Pbc proteins leads to the nuclear import of the former, which lack a nuclear localization signal, and prevents the nuclear export of the latter (Abu-Shaar et al., 1999; Berthelsen et al., 1999). Because Pbc uses different surfaces to interact with Hox and Meinox proteins, Pbc-Hox and Meinox-Pbc molecular interactions direct the formation of Meinox-Pbc-Hox trimers. Such trimeric complexes recognize a split, 16-bp sequence on the regulatory regions of target genes (Ferretti et al., 2000; Jacobs et al., 1999; Ryoo et al., 1999). Moreover, Meinox proteins are important in stabilizing Pbc members. For example, Hth is required to maintain the level of the Pbc protein Exd in *D. melanogaster* (Kurant et al., 2001) and overexpression of dominant negative Meis derivatives reduce the level of Pbx proteins in higher vertebrates and zebrafish (Capdevila and Belmonte, 1999; Choe et al., 2002; Mercader et al., 1999; Waskiewicz et al., 2001), whereas overexpression of Prep1 in mammalian cells increases the level of Pbx proteins (Longobardi and Blasi, 2003).

A total of 14 *hox* paralogs (11 in the mouse), 2 *pbx*, 3 *meis* and 2 *prep* genes are expressed in zebrafish hindbrain (Moens and Prince, 2002). The inactivation of *pbx4/lazarus* (*lzar*) in

zebrafish leads to a phenotype that is characterized by embryonic death at 6–7 days post-fertilization (dpf) with major developmental defects, in particular in hindbrain segmentation and cranial neural crest determination (Pöpperl et al., 2000). This phenotype closely resembles that of the mouse *Pbx1*-null mutant (Selleri et al., 2001) because, in both cases, major developmental defects are observed in the cartilages arising from the second branchial arch. In zebrafish, elimination of hindbrain-expressed Pbx proteins (Pbx2 and Pbx4) uncovers a hindbrain ground state in which rhombomeres 2 to 6 (r2–r6) acquire an r1 identity (Waskiewicz et al., 2002). In *Xenopus*, zebrafish and chicken, the role of Meis proteins has been investigated by overexpression and dominant-negative mutant approaches (Dibner et al., 2001; Mercader et al., 1999; Salzberg et al., 1999; Vlachakis et al., 2001; Waskiewicz et al., 2001). However, the specific role of individual Meis or Prep proteins is unknown.

Prep1 was identified as a protein that copurifies with several Pbx proteins in human cells, and Prep2 was identified from a search of the human genome sequence and cloned subsequently (Berthelsen et al., 1998a; Berthelsen et al., 1998b; Fognani et al., 2002; Haller et al., 2002). Together, they form a subgroup of Meinox proteins that share ~80% overall amino acid sequence identity. By contrast, the Meis and Prep proteins share high amino acid sequence conservation only in specific domains (Fognani et al., 2002). An additional difference between Prep and Meis might lie in Hox proteins binding activity. Vertebrate Meis associates in vitro with Hox9–Hox13, which increases the DNA-binding specificity of the Meis-Hox complex (Shen et al., 1997); no such properties appear to be present in Prep1 (Thorsteinsdottir et al., 2001). Whereas *prep1.1* and *prep1.2* are expressed almost ubiquitously in zebrafish, at least in early developmental stages up to 24 hpf (Choe et al., 2002), the expression of *meis* genes is more restricted (Biemar et al., 2001; Waskiewicz et al., 2001). However, both Meis and Prep bind to Pbx proteins, need Pbx for nuclear localization and prevent export of Pbx from the nucleus.

In the present investigation we have studied the functional role of the *prep1.1* gene during early zebrafish development using antisense morpholino technology. We demonstrate that *prep1.1* is necessary for histogenesis of the pharyngeal skeleton and, interacting with Pbc, is crucial for hindbrain patterning. In addition, our results support the idea that segmentation of the hindbrain and pharyngeal arches are independent processes.

Materials and methods

Characterization and radiation hybrid-panel mapping of *prep1.1*

We screened the Genbank database for a zebrafish expressed sequence tag (EST) that contained an open reading frame (ORF) that encoded a polypeptide homologous to human PREP1. One of the clones matching the criteria, fc13f10, was obtained from RZPD (Berlin) and sequenced completely. Sequence analysis of this EST revealed an ORF encoding a protein of 433 amino acids that contained two HR domains and one TALE homeodomain (Fig. 2A). Sequence comparison and phylogenetic reconstruction showed that the fc13f10 ORF is more similar to human PREP1 than to its paralogue PREP2 (Fig. 1A); for this reason the zebrafish fc13f10 EST was called *prep1.1*.

To determine the position of *prep1.1* onto the zebrafish genetic map we used the Zebrafish/Hamster Radiation Hybrid Panel (Goodfellow T51 panel, Invitrogen). The panel was screened by PCR using primers 5'-TCAACAGAGGCATCTAAAAGC-3' and 5'-GTCGCTGACGT-CATAAACCC-3', and 125 ng template, 100 nM each primer, 100 μM each dNTP, 2 mM MgCl₂ and 1.25 units Taq DNA Polymerase (Promega). Thirty five cycles of PCR were completed: 94°C for 30 seconds, 59°C for 30 seconds, 72°C for 30 seconds. The retention profile of the PCR reaction was placed by the RH Instant Mapper program (<http://134.174.23.167/zonrhmapper/instantMapping.htm>) at 1894 cRay on chromosome 9, between meiotic SLP markers z4168 (796 cRay, 48.7 cM) and z6663 (2071 cRay, 48.7 cM).

RNA constructs and microinjections

To create the *prep1.1*-deletion constructs (Fig. 2A), the full-length *prep1.1* cDNA (RZPD clone MPMGp609C2025Q8) was dissected by PCR amplification. The primers used to prepare *prep1.1* ΔHR1-2 cDNA, in which HR1-2 (Meis family Homology Regions 1 and 2) are deleted, were:

5'-cgggatccCATTTTGAATATGATGGCTGC-3'
 5'-gaagatccCATGACCAGTTGTCCAACC-3'
 5'-gaagatctTTGTGTTTGTGGTTCATTGG-3'
 5'-cgggatccGTCGCTGACGTCTAAACCC-3'

The primers used to amplify *prep1.1* ΔHD cDNA, in which the homedomain (HD) is deleted, were:

5'-cgggatccCATTTTGAATATGATGGCTGC-3'
 5'-gaagatctTCAACAGAGGCATCTAAAAGC-3'
 5'-gaagatctTCCCGAAGAACTCCAAGTCC-3'
 5'-cgggatccGTCGCTGACGTCTAAACCC-3'

The primer used to prepare full coding *prep1.1* cDNA, which lack 5' and 3' non-coding ends, were:

5'-cgggatccCATTTTGAATATGATGGCTGC-3'
 5'-cgggatccGTCGCTGACGTCTAAACCC-3'

In each case, *Bam*HI and *Bgl*III sites are underlined. Constructs were subcloned in *Bam*HI sites of *pCS2+* and *pCS2+GFP* plasmid vectors and sequenced. For microinjection of mRNAs, plasmids containing coding sequences were linearized, and sense-strand capped mRNAs synthesized using SP6-dependent mMessage mMachin kit (Ambion). Subsequently, mRNAs were purified, tested by agarose-gel electrophoresis, diluted in PBS and microinjected into fertilized embryos at the one-cell stage. The amount of mRNA injected was determined by measuring the diameter of the drop injected. To confirm that mRNA cause no nonspecific effects during embryogenesis, control embryos were also injected with an mRNA encoding green fluorescent protein (GFP).

Morpholino antisense oligonucleotides were obtained from Gene Tools. The sequences of morpholinos used were as follows:

prep1.1-MOa, 5'-TGGACACAGACTGGGCAGCCATCAT-3' (fluorescein tagged at 3' end); *prep1.1*-MOb, 5'-GCCAACTGCCAACTGGGACATTAT-3';

pbx4-MO, 5'-GATCATCCATAATACTTTTGTAGCCG-3';

negative control-MO, 5'-CCTCTTACCTCAGTTACAATTATA-3' (fluorescein tagged at 3' end).

The *pbx2*-MO has been described (Waskiewicz et al., 2002). The stock solution was diluted to working concentrations of 0.5–3.0 mg ml⁻¹ in Danieau solution [58 mM NaCl, 0.7 mM KCl, 0.4 mM MgSO₄, 0.6 mM Ca(NO₃)₂, 5 mM HEPES pH 7.6], before injection into the yolk of embryos at the one-cell stage. For the rescue experiment, *prep1.1*-MOb was co-injected with synthetic *prep1.1* mRNA. To test the capacity of *prep1.1*-MOa to block translation, zebrafish eggs were injected with 25 pg of *prep1.1*-GFP mRNA and 2 ng of *prep1.1*-MOa (directed against the start codon and fluorescein tagged at the 3' end). The embryos were then fixed at 80% epiboly and GFP expression tested using anti-GFP antiserum (Biotac). Lack of staining in embryos co-injected with *prep1.1*-GFP and *prep1.1*-MOa, confirmed the specific targeting.

Table 1. Results of microinjection experiments

Construct injected	Amount injected	Injected/survived	Abnormal phenotype	Type	Wild-type phenotype
<i>prep1.1</i> - MOa	3 ng	141/129	129 (100%)	S	0 (0%)
<i>prep1.1</i> - MOa	2 ng	101/96	90 (93.8%)	S	6 (6.2%)
<i>prep1.1</i> - MOb	2 ng	113/106	104 (98.1%)	S	2 (1.9%)
<i>prep1.1</i> - MOb	1 ng	107/79	70 (88.6%)	S	9 (11.4%)
<i>prep1.1</i> - MO _a + <i>prep1.1</i> - MOb	0.5 + 0.5 ng	93/90	90 (100%)	S	0 (0%)
<i>prep1.1</i> -GFP mRNA + <i>prep1.1</i> - MOb	50 pg + 2 ng	135/121	55 (45.5%)	S	66 (54.5%)
<i>pbx4</i> -MO	2 ng	144/132	128 (97%)	<i>lzt</i>	4 (3%)
<i>prep1.1</i> -GFP mRNA + <i>pbx4</i> -MO	10 pg + 3 ng	53/45	44 (98%)	<i>lzt</i>	1 (2%)
<i>prep1.1</i> -GFP mRNA + <i>pbx4</i> -MO	10 pg + 6 ng	55/34	34 (100%)	<i>lzt</i>	0 (0%)
Control MO	2 ng	46/43	0 (0%)	-	43 (100%)
<i>prep1.1</i> mRNA	100 pg	62/44	25 (56.8%)	P	19 (43.2%)
<i>prep1.1</i> mRNA	50 pg	46/35	18 (51.4%)	P	17 (48.6%)
<i>prep1.1</i> -GFP mRNA	100 pg	34/19	11 (57.9%)	P	8 (42.1%)
<i>prep1.1</i> -GFP mRNA	50 pg	87/72	43 (59.7%)	P	29 (40.3%)
<i>prep1.1</i> -GFP mRNA	10 pg	50/43	1 (2.3%)	P	42 (97.7%)
<i>prep1.1</i> ΔHD-GFP mRNA	50 pg	40/35	15 (42.9%)	P	20 (57.1%)
<i>prep1.1</i> ΔHR1-2-GFP mRNA	50 pg	28/27	0 (0%)	-	27 (100%)

Each row represents one experiment with the same batch of mRNA and/or morpholino (MO). Embryos injected at the one-cell stage were observed at 24 hpf and abnormal phenotypes classified either as S (*spacehead*-like) (Abdelilah et al., 1996), P (posteriorized) and *lzt* (*lazarus*) (Pöpperl et al., 2000). Injection of 10 pg of *prep1.1*-GFP mRNA had no significant effect on the phenotype, whereas the maximum effect was reached with 50 pg. By contrast, injection of 50 pg of *prep1.1*ΔHR-GFP, which encodes a Prep1.1 derivative that is not translocated to the nucleus (see Fig. 2), did not affect the phenotype. The embryos referred to in this Table are different from those in Figs 4-7.

RT-PCR

Total RNA was extracted from ~100 frozen embryos at each developmental stage and from dissected ovaries using TRIzol (Gibco), purified with DNaseI and quantified by agarose-gel electrophoresis. mRNA was then retrotranscribed and amplified with the Access RT-PCR System kit (Promega) using oligos specific for either *prep1.1* (5'-CTCTTTTCCCTCTCCGGCT-3' and 5'-ATGAATCCTCAGCAGCTGGA-3'), which gave a 580-bp cDNA product, or *β-actin* (5'-TGTTTTCCCTCCATTGTTGG-3' and 5'-TTCTCCTTGATGTCACGGAC-3'), which resulted in a 560-bp cDNA product.

Cell extracts and immunoblotting

After dissection, 100 zebrafish embryos were resuspended in 60 μl lysis buffer (10 mM HEPES pH 7.9, 30 mM KCl, 1.5 mM MgCl₂, 1 mM DTT, 0.5 mM PMSF, 1 mM Na₂S₂O₅), kept in ice for 10 minutes and lysed with TritonX-100 to a final concentration of 0.1%. The nuclei were washed and the cell debris collected by centrifugation. The supernatant was removed into a new tube, added to 0.11 vol of 0.3 mM HEPES pH 7.9, 1.5 mM MgCl₂ and centrifuged. The resulting supernatant corresponds to the cytoplasmic extract (CE). Nuclear extract (NE) was prepared by resuspending the nuclear pellet in 30 μl of 20 mM HEPES pH 7.9, 25% glycerol (v/v), 0.42 M NaCl, 1.5 mM MgCl₂, 1 mM DTT, 0.5 mM PMSF, 1 mM Na₂S₂O₅, and incubating at 4°C with shaking for 30 minutes. The extracts were cleared by centrifugation. Extracts (30 μg of NE and 60 μg of CE) were separated by 10% SDS-PAGE and blotted to PVDF membrane (Millipore).

Immunoblotting analysis was performed with the anti pan-Pbx antibodies (1:5000) (Pöpperl et al., 2000), kindly provided by H. Pöpperl. The final detection utilized the Dura chemoluminescent kit (Pierce).

Immunohistochemistry and histology

Cartilage staining

Larvae were fixed overnight in 4% buffered *p*-formaldehyde, rinsed in distilled water and stained overnight in a 0.1% Alcian blue solution. Larvae were then cleared by washing sequentially in 3% hydrogen peroxide and 70% glycerol, and whole mounted.

Whole-mount in situ hybridization

Embryos were fixed in 4% buffered *p*-formaldehyde. RNA in situ hybridizations were performed essentially as reported in (Thisse et al., 1993). Digoxigenin and fluorescein-labelled antisense probes were synthesized from cDNAs of *prep1.1* (RZPD clone MPMGp609C2025Q8), *krox20* (Oxtoby and Jowett, 1993), *pax6.1* (Puschel et al., 1992), *pax2.1* (Krauss et al., 1991), *islet1* (Korzh et al., 1993), *snail1* (Thisse et al., 1993), *foxb1.2/mariposa* (Moens et al., 1996), *hoxb1b* and *hoxb1a* (McClintock et al., 2001), *hoxa2* and *hoxb2* (Prince et al., 1998), *dlx2* (Akimenko et al., 1994), *col2a1* (Sachdev et al., 2001) and *myoD* (Weinberg et al., 1996). Results of the hybridizations were analyzed statistically using Chi-square analysis.

Immunohistochemistry

Antibody staining of whole-mounted embryos with acetylated tubulin, RMO-44 and Zn5, was performed essentially as described by (Abdelilah et al., 1996; Piotrowski and Nüsslein-Volhard, 2000; Waskiewicz et al., 2001), respectively.

Detection of apoptotic cell death

For a preliminary analysis of cell death, embryos were stained with the vital dye acridine orange (acridinium chloride hemi-zinc chloride; Sigma) (Abrams, 1999). Embryos were incubated for 10-15 minutes in 5 μg ml⁻¹ acridine orange, washed two times for 5 minutes in Fish Water (60 mg l⁻¹; Instant Ocean) and observed under a microscope (Leica MZFLIII) using a green filter set to reveal labelled cells undergoing cell death. For further analysis, apoptosis was detected by terminal transferase dUTP nick-end labelling (TUNEL), as previously described (Williams et al., 2000).

Retrograde labelling

RSNs were revealed by retrograde labelling from the spinal cord of 3- and 5-day-old larvae, as described (Alexandre et al., 1996). Labelled brains were dissected free of surrounding larval tissues, mounted in 50% glycerol in PBS and visualized by epifluorescence with a compound microscope (Leica Diaplan) using a Texas-red filter.

Image acquisition and elaboration

Subcellular dynamics of Prep1.1-GFP constructs were visualized,

acquired and elaborated with the Bio-Rad Radiance 2000 confocal system. All other pictures were acquired from microscope phototubes using a Leica DC500 photcamera and processed with Adobe Photoshop software.

Results

prep1.1 mRNA expression pattern

Previous studies have documented the occurrence of *prep1.1* transcripts in zebrafish embryos from the earliest developmental stages to 25 hpf, which implies that *prep1.1* mRNA is laid down maternally (Choe et al., 2002; Waskiewicz et al., 2001). Our RT-PCR analysis shows that *prep1.1* cDNA could be amplified from total RNA of mature ovaries and embryos at all stages studied, from 2 cells to larval day 4 (Fig. 1B), which confirms the occurrence of maternally expressed *prep1.1* mRNA in zebrafish embryos. Transcripts of *prep1.1*, revealed with an anti-sense probe, were distributed ubiquitously in the embryo up to 24 hpf (Fig. 1C-G), whereas no labelling was detected with a sense probe (not shown). However staining in the trunk and tail, was already weaker at 24 hpf, markedly reduced at 48 hpf (Fig. 1H) and had completely disappeared by 72 hpf (Fig. 1I). At 72 hpf, labelling was limited to the head, predominantly in the brain and otic vesicles, the latter representing the posteriormost boundary of *prep1.1* expression. Hence, *prep1.1* transcripts were initially spread throughout the embryo, but became restricted to the head in later developmental stages.

Prep1.1 may be translocated to the nucleus from gastrulation onwards in the whole embryo

Prep1.1 is a cofactor in transcriptional regulation, so its presence in the nucleus is a prerequisite for its activity. To determine the timing and regulation of the nuclear localization of Prep1.1, we injected fertilized eggs with 10 pg of *prep1.1-GFP* mRNA, a dose that did not alter the phenotype (Table 1) but allowed the subcellular localization of the fluorescent

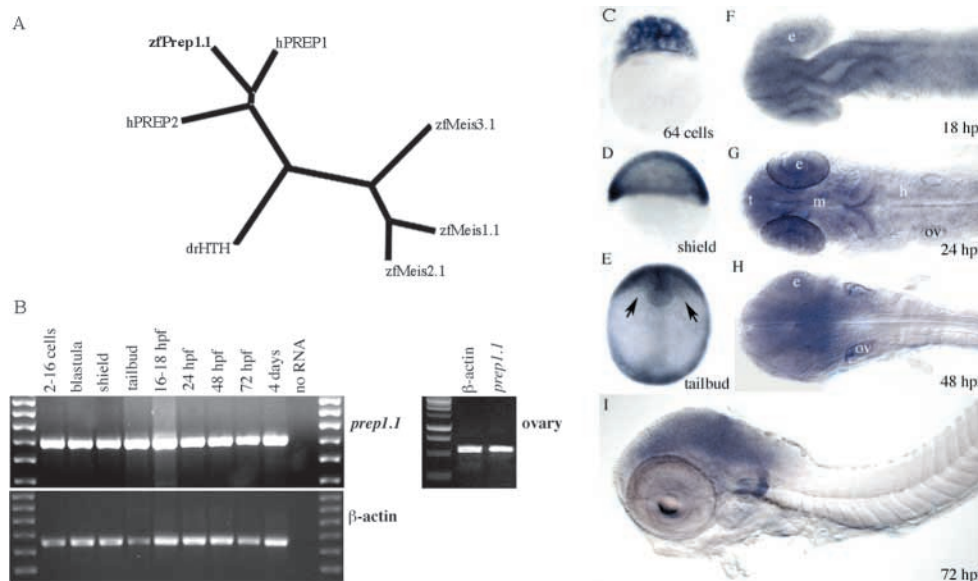
protein to be tracked directly in live embryos. We found that Prep1.1-GFP localized in the cytoplasm at early developmental stages and that its nuclear import began during the blastula period. In particular, the fluorescent protein was exclusively cytoplasmic during the high stage (not shown) but soon after, during the sphere stage, was traced both to the cytoplasm and nucleus (Fig. 2B). Then, from 30% to 50% epiboly, Prep1.1-GFP became predominantly nuclear (Fig. 2C) and, at the beginning of gastrulation, was almost exclusively localized to the nucleus (Fig. 2D). An identical pattern was observed after injection of *prep1.1ΔHD-GFP* mRNA (Fig. 2I), which encodes a GFP-linked derivative of Prep1.1 that lacks the homeodomain (Fig. 2A). Conversely, injection of *prep1.1ΔHR-GFP* mRNA, which encodes a GFP-linked Prep1.1 derivative that lacks HR1 and HR2 Pbx-binding regions, resulted in the restriction of the fluorescent product to the cytoplasm (Fig. 2J). Incidentally, this also excluded the possibility that the nuclear localization of Prep1.1-GFP was influenced by the GFP moiety. On the basis of these results we conclude that (1) the mechanisms required for the nuclear translocation of Prep1.1 are fully effective at the onset of gastrulation in the whole embryo, and (2) as for other Meinox proteins, the Pbx-binding region, but not the homeodomain, is required for its nuclear import.

Prep1.1 nuclear translocation involves Pbx4

The nuclear transport of Meinox proteins is a highly conserved mechanism requiring the formation of Pbx-Meinox complexes that are translocated to the nucleus because of a nuclear-localization signal in the Pbx homeodomain (Abu-Shaar et al., 1999; Berthelsen et al., 1999). Pbx4/Lzr is the Pbx member with higher levels of expression during zebrafish embryogenesis (see Fig. 2K) (Waskiewicz et al., 2002), indicating that it might be the most important partner of Prep1.1 in early development. To determine whether the two proteins interacted during embryogenesis, we examined the subcellular localization of Prep1.1-GFP in live embryos in which *pbx4* expression was repressed using a *pbx4*

Fig. 1. Expression of *prep1.1* transcripts during development.

(A) Dendrogram, obtained using the ClustalW program, of zebrafish Meis1.1, Meis2.1, Meis3.1 and Prep1.1, human PREP1 and PREP2 (hPREP1 and hPREP2), and *Drosophila* Homotorax (drHTH) protein sequences. (B) RT-PCR amplifies *prep1.1* transcripts in zebrafish embryos at all stages from 2-16 cells to 4 dpf, and in ovaries of mature females. (C-I) RNA in situ hybridization of wild-type embryos. (C-F) *prep1.1* transcripts are distributed ubiquitously up to 18 hpf. Arrows in E indicate head mesoderm. (G-I) From 24 hpf onwards *prep1.1* transcripts concentrate in the head and become restricted to the region rostral to the otic vesicles (ov) at 72 hpf. Embryo in D is in lateral view with ventral to the left. Embryo in E is in frontal view. Embryos in F-H are in dorsal view and embryo in I is in lateral view. e, eye; m, midbrain; h, hindbrain; t, telencephalon.



morpholino. The fact that the phenotype of nearly all embryos injected with 2 ng of *pbx4*-MO at the one-cell stage was altered, proved the effectiveness of the morpholino treatment (Table 1). The specificity of the effects produced by the *pbx4*-MO was demonstrated by the observation that *pbx4* morphants displayed morphological anomalies (Fig. 3I) and impaired expression patterns of molecular markers (see below), identical to those observed in the *lzf* mutant (Pöpperl et al., 2000). We found that in embryos that received 2-6 ng of *pbx4*-MO and 10 pg of *prep1.1-GFP* mRNA, the fluorescent protein was translocated to the nucleus with the same temporal pattern in both *pbx4*-MO-treated embryos and untreated siblings (Fig. 2E-G). But, importantly, in all *pbx4* morphants a significant amount of Prep1.1-GFP was traced to the cytoplasm in stages when it was restricted mostly to the nucleus in the controls (Fig. 2D,G). This provided evidence that Pbx4 is involved in the nuclear transport of Prep1.1. Moreover, the nuclear signal was not abolished in *pbx2/pbx4* double morphants (not shown),

suggesting that maternal Pbx4, which is still present at 10 hpf in *pbx4/lzf* homozygous mutants (Waskiewicz et al., 2002), was responsible of the residual nuclear import of Prep1.1-GFP.

prep1.1 inactivation affects the levels of both Pbx2 and Pbx4

Hth/Meis/Prep proteins influence the subcellular localization (Abu-Shaar et al., 1999; Berthelsen et al., 1999) and the stability of their Exd/Pbx partners (Kurant et al., 2001; Waskiewicz et al., 2001; Longobardi and Blasi, 2003). Because this indicates that Prep1.1 interacts with Pbx4 and, possibly, other Pbx proteins, we asked whether Prep1.1 might affect the levels and localization of Pbx proteins. To this purpose, we performed an immunoblot analysis, using a pan-Pbx antibody (Pöpperl et al., 2000), to test cytoplasmic and nuclear extracts of wild-type and *prep1.1*-MO-treated embryos at 24 hpf. As a control, we employed human Pbx1a and Pbx1b cotranslated in vitro with human Prep1. The pan-Pbx antibodies identified the 47×10^3 and 39×10^3 M_r bands expected for the two Pbx proteins (Fig. 2K). Moreover, the same two bands were also identified in extracts from human HEK cells, whereas a species of $\sim 38 \times 10^3$ M_r was revealed in an extract from mouse testis (Wagner et al., 2001). When tested with the zebrafish extracts, the pan-Pbx antiserum revealed two major bands with mobilities that matched the electrophoretic migration of in vitro translated mouse Pbx1b (38.5×10^3 M_r) and Pbx1a (46.5×10^3 M_r). This pattern is identical to that obtained by Waskiewicz et al. (Waskiewicz et al., 2002) in identifying Pbx2

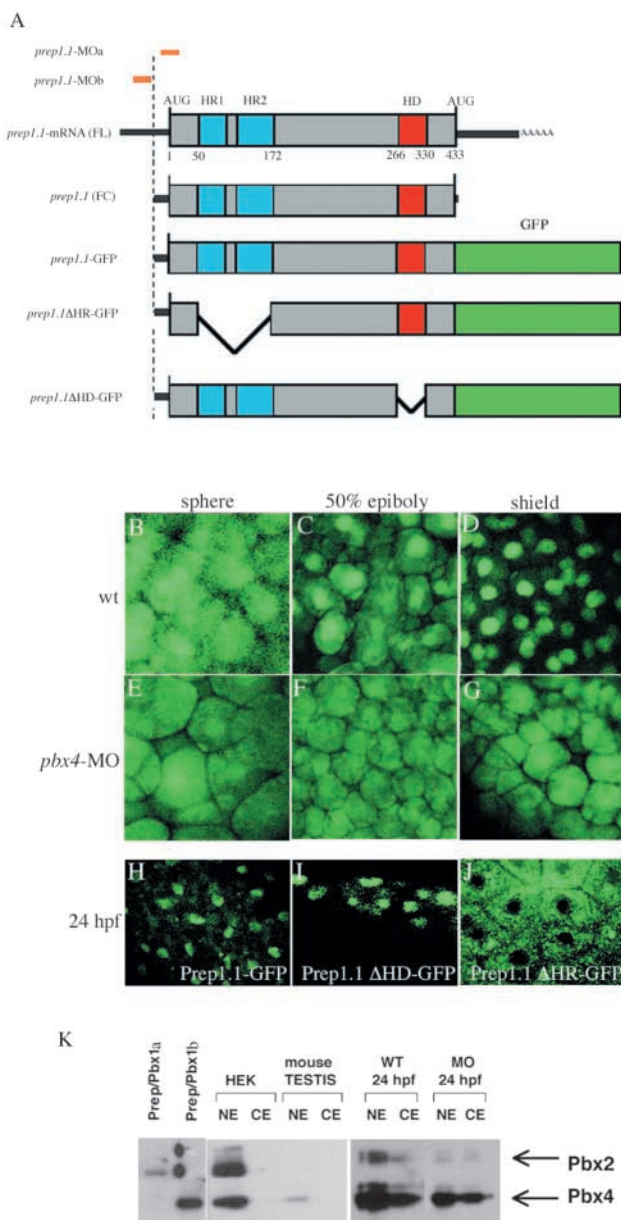
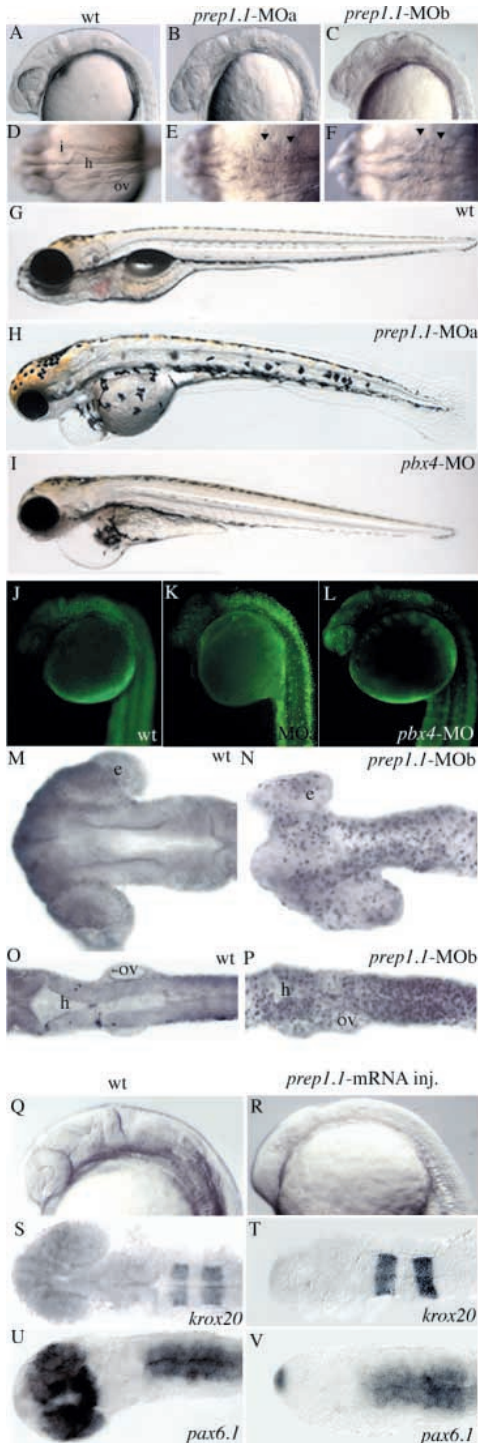


Fig. 2. Subcellular localization of Prep1.1-GFP. (A) Full-length zebrafish *prep1.1*, as sequenced from the EST fc13f10, is represented with the Meis family homology regions (HR1 and HR2) in blue and the homeodomain homology region (HD) in red. The positions of the morpholinos (MOs) relative to the cDNA sequence are indicated by orange bars. *prep1.1* constructs, with GFP coding sequence in green, are also shown. *prep1.1*-MOb inactivates endogenous, full-length mRNA but not the full-coding constructs. (B-J) Subcellular localization of Prep1.1-GFP chimeric proteins. (B-D,H) In a wild-type embryo injected with 10 pg of *prep1.1*-GFP mRNA, Prep1.1-GFP, which is cytoplasmic at the high stage (not shown), is translocated to the nucleus from the sphere stage onwards. Starting from the shield stage, the fluorescent protein is restricted mostly to the nucleus. (E-G) In a *pbx4* morphant injected with 6 ng *pbx4*-MO and 10 pg *prep1.1*-GFP mRNA, Prep1.1-GFP is also translocated to the nucleus from the sphere stage onwards, but significant amounts are detected in the cytoplasm in all subsequent stages. (I,J) In wild-type embryos, Prep1.1ΔHD-GFP, a derivative lacking the homeodomain, is translocated normally to the nucleus (I), whereas Prep1.1ΔHR-GFP, a derivative lacking the Meis homology region is not (J). (B-D,H) and (E-G) are from the same wild-type and *pbx4* morphant embryos, respectively. (K) Western blot of extracts from 24 hpf zebrafish embryos. The left panel is a control blot to assess the migration of two Pbx proteins, mPbx1a and mPbx1b, of known molecular weight and antibody specificity. The two proteins, which are recognized specifically by the pan-Pbx antibody, were translated in vitro with hPrep1 in a rabbit reticulocyte system. The middle panel is another control using nuclear extracts (NE) and cytoplasmic extracts (CE) of either human HEK293 cells or mouse testis. The right panel shows the immunoblotting analysis of NE and CE from wild-type zebrafish embryos at 24 hpf and following injection of *prep1.1*-MOb. The migration of Pbx2 and Pbx4 (arrows) is inferred on the basis of the M_r of the bands, and observation of the identical pattern elsewhere (Waskiewicz et al., 2002). A pan-Pbx antibody (Pöpperl et al., 2000) was used throughout.

and Pbx4. Both species were more abundant in NEs than CEs and, importantly, all the bands were much more intense in extracts from wild-type embryos than *prep1.1* morphants. As the assay was standardized by loading an equal amount of protein and by Ponceau staining of the gel (not shown), it appears that suppression of *prep1.1* expression caused a significant decrease of the concentration of Pbx2 and Pbx4 in both nucleus and cytoplasm. This is consistent with the possibility that Prep1.1 stabilizes and increases the nuclear localization of different Pbx proteins.



Effects of *prep1.1* mRNA inactivation and overexpression

It has been shown that appropriate amounts of antisense morpholinos injected into zebrafish embryos at the one-cell stage might repress the expression of both maternal and zygotic genes (Nasevicius and Ekker, 2000). Hence, as the first step in investigating the functional role of *prep1.1* during early embryonic development we adopted the morpholino approach to examine the phenotypic effects induced by *prep1.1* inactivation. We used two different morpholinos, complementary to either the initial 25 bp of the translated region (MOa) or a 25-bp sequence from the 5'-untranslated region (MOb) of *prep1.1* mRNA (Fig. 2A). Embryos that received either *prep1.1*-MOs developed normally, both morphologically and temporally, up to early somitogenesis. However, at the 15-somite stage (16.5 hpf), cell death was apparent in the form of an opacity in the neuroectoderm. The effects of the two morpholinos were indistinguishable, dose-dependent and synergistic: 2-3 ng of either morpholino injected separately or 0.5 ng of each injected in combination, modified the phenotype of virtually all embryos treated (Table 1). One-day old morphants were characterized by a prominent area of degeneration, which was clearly visible bilaterally both inside and outside the CNS at the level of the hindbrain (Fig. 3B,C,E,F). Morphant embryos were impaired in motor coordination, so that most were unable to exit from the shell. At 5 dpf, the morphant embryos had small heads and eyes, and atrophic pectoral fins; they lacked jaws and a recognizable swim bladder and displayed an abnormal distribution of melanocytes and pericardial edema (Fig. 3H). The morphant embryos did not survive after 6-7 dpf.

We next investigated the effects of Prep1.1 overexpression by injecting one-cell stage embryos with either 50 pg or 100 pg of *prep1.1* mRNA. Embryos injected with either dose developed normally beyond gastrulation, but the phenotype of >50% of the treated embryos was markedly affected at 24 hpf (Table 1). Injection of 50 pg *prep1.1* mRNA induced two main

Fig. 3. The phenotype of *prep1.1* morphants is characterized by apoptosis. (A-I) 24-hpf and 5-dpf embryos. (B,C,E,F) Embryos injected with either *prep1.1*-MOa or *prep1.1*-MOb have similar brain phenotypes, characterized by alterations in brain morphology and widespread cell death, which is clearly visible as a higher opacity that is particularly evident at the level of the hindbrain (arrowheads in E,F). (H) *prep1.1* morphants are characterized by small head and eyes, lack of jaws, abnormal distribution of melanocytes and delayed reabsorption of the yolk sac. (I) *pbx4* morphants are characterized by small head and eyes and reduced jaws. Both *prep1.1* and *pbx4* morphants display a swollen pericardium and lack an inflated swim bladder. (A-C,G-I) are lateral, and (D-F) are dorsal views, with anterior to the left. (J-L) Acridine orange staining reveals widespread cell death in *prep1.1* morphants, but not in wild-type embryos and *pbx4* morphants. Embryos are in lateral views. (M-P) TUNEL labelling reveals intense DNA fragmentation in the brain of *prep1.1* morphants at the 22-somite stage, which is more pronounced in the hindbrain. Embryos are in dorsal views with anterior to the left. (Q-V) Injection of *prep1.1* mRNA posteriorizes the zebrafish embryo. Visual inspection (Q,R), and in situ hybridization with *krox20* (S,T) and *pax6.1* (U,V) antisense probes reveals that embryos injected with *prep1.1* mRNA (R,T,V) have a reduced forebrain compared to uninjected embryos (Q,S,U). e, eye; h, hindbrain; I, isthmus; ov, otic vesicle.

phenotypes in ~50% of embryos, both characterized by a shortening of the head, as evidenced by a decreased distance between the eye and the otic vesicle (Fig. 3R). Most of these embryos had a phenotype in which the eyes were closer one to another but still distinct, whereas a few exhibited a more severe phenotype that was characterized by a single cyclopic eye. In situ hybridization with a *krox20* antisense probe showed that the hindbrain was unaffected (Fig. 3T) but a *pax6.1* probe revealed a strong reduction of the forebrain (Fig. 3V). Similar effects were observed in embryos treated with 50 pg of *prep1.1ΔHD-GFP* mRNA, encoding a GFP-linked Prep1.1 derivative lacking the homeodomain (Table 1), but in this case most embryos were cyclopic. This indicates that deletion of the homeodomain does not impair but rather increases the activity of Prep1.1, reminiscent of the finding that deletion of the PREP1 homeodomain might enhance the transcriptional activity of mammalian PBX1-HOXB1-PREP1 complexes (Berthelsen et al., 1998b). Moreover, embryos that received 100 pg of *prep1.1* mRNA, displayed a even more extreme phenotype, characterized by the absence of eyes and a marked reduction of all head structures. Conversely, overexpression of *prep1.1ΔHR-GFP* mRNA, which encodes a GFP-linked Prep1.1 derivative that lacks the HR1 and HR2 regions, had no phenotypic consequences (Table 1). This indicates that, as with other members of the Meinox family (Choe et al., 2002), the Pbx-interacting domain is crucial to Prep1.1 activity. In summary, the results of the overexpression of *prep1.1* in zebrafish closely resemble those obtained in *Xenopus* in which the overexpression of *meis3* causes caudalization of anterior neural tissue (Salzberg et al., 1999; Dibner et al., 2001).

To verify the specificity of the morpholinos, we checked whether the mutant phenotype was rescued by coinjecting MOB with a *prep1.1*-expressing mRNA. To this purpose, we used an mRNA (*prep1.1-GFP* mRNA) that encodes wild-type Prep1.1 linked to GFP, so that expression of the chimeric protein could be ascertained visually in the embryos. This experiment could be devised for two reasons: first, when overexpressed in zebrafish embryos, Prep1.1-GFP and Prep1.1 produced qualitatively and quantitatively identical effects (Table 1), indicating that the activity of the chimeric protein was not significantly affected by the GFP moiety; second, because the *prep1.1*-MOB was complementary to a sequence of the 5' UTR, it blocked the endogenous *prep1.1* mRNA but not the microinjected synthetic *prep1.1-GFP* mRNA (Fig. 2A). As shown (Table 1), The number of embryos displaying the wild-type phenotype increased from <2% of those injected with 2 ng of *prep1.1*-MOB alone to >54% of those that received in addition 50 pg of *prep1.1-GFP* mRNA, thereby demonstrating that Prep1.1-GFP was effective in rescuing the mutant phenotype. Thus, it appears that the *prep1.1*-MOs used in the present investigation inhibited specifically the expression of *prep1.1*.

Neural degeneration in *prep1.1* morphants is caused by apoptosis

Visual inspection of *prep1.1* morphants revealed a pronounced process of degeneration that started during early somitogenesis and peaked at about 24–36 hpf. Staining with the vital dye acridine orange showed a major increase in cell death in *prep1.1* morphants. Although this occurred principally in the CNS, in particular the hindbrain and spinal cord, it was also

significant in other tissues (Fig. 3K). By contrast, acridine orange staining was inconsistent in wild-type embryos and *pax4* morphants (Fig. 3J,L). To establish whether cell death induced by *prep1.1* inactivation was due to apoptosis, the embryos were analyzed by in situ TUNEL assay to detect DNA fragmentation. As shown in Fig. 3 (Fig. 3N,P) TUNEL labelling was evident throughout the brain of *prep1.1*-MOB-treated embryos, especially in the hindbrain, but was limited in the brains of controls (Fig. 3M,O). Therefore, we conclude that the pronounced cell death induced by *prep1.1* inactivation was due primarily to apoptosis.

prep1.1 knockdown disrupts hindbrain segmentation

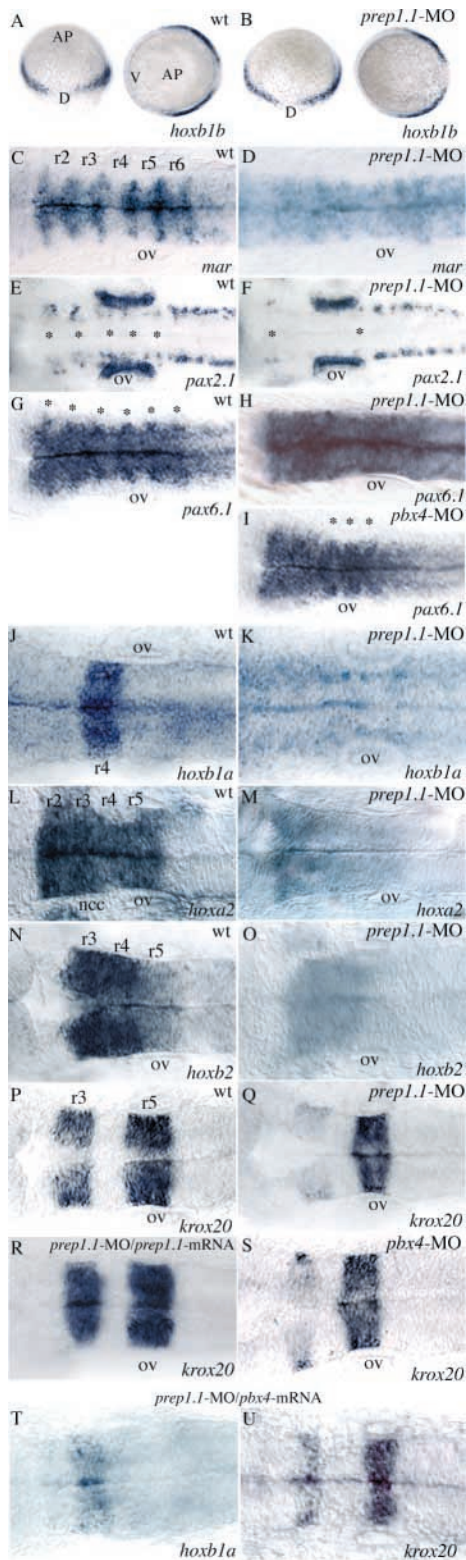
In zebrafish, Pbx proteins are essential for hindbrain development (Waskiewicz et al., 2002), but overexpression of wild-type and dominant-negative Meis proteins also support the idea of an important role of Meinox proteins in this process (Choe et al., 2002; Vlachakis et al., 2001). As both the morphological inspection and TUNEL analysis showed that the hindbrain is significantly affected in *prep1.1* morphants, we addressed the role of *prep1.1* in hindbrain development by analysing the effects of its knockdown on the expression of several hindbrain markers. The results were compared to those observed in mutants that lack Pbx proteins (Pöpperl et al., 2000; Waskiewicz et al., 2002) and embryos treated with a *pax4* morpholino.

In zebrafish, *hoxb1b* is indispensable for normal segmentation of the hindbrain (McClintock et al., 2001), and the onset of its expression represents the initial step of hindbrain patterning (Waskiewicz et al., 2002). Hence, we first checked whether the expression of *hoxb1b* was altered in *prep1.1* morphants. We observed that expression of this gene was indistinguishable in wild-type and *prep1.1*-MOB-injected embryos (Fig. 4A,B). Because expression of *hoxb1b* is also unaffected by eliminating both *pax2* and *pax4* (Waskiewicz et al., 2002), it appears that neither Prep1.1 nor Pbx proteins are involved in the regulation of this gene.

We then investigated the effects of *prep1.1* knockdown on the expression of *foxb1.2/mariposa* and *pax6.1*, two genes that depict hindbrain segmentation by outlining rhombomere boundaries (Moens et al., 1996; Choe et al., 2002). As shown in Fig. 4 (Fig. 4C,D,G,H), *prep1.1* knockdown caused the loss of the six clear-cut boundaries (from r1-r2 to r6-r7), evidenced by the expression of these two genes in wild-type embryos. By contrast, in *pax4* morphants (Fig. 4I) *pax6.1* expression revealed that hindbrain segmentation was indistinct rostrally but remained clearly identifiable in the three caudal boundaries (from r4-r5 to r6-r7). This agrees with the expression pattern of *pax6.1* observed in embryos that express ectopically a dominant negative derivative of *pax4* (Choe et al., 2002), and correlates with the fact that in mutants such as *lzf* (Pöpperl et al., 2000) and *MZlzf* (which lacks both maternal and zygotic *pax4*) (Waskiewicz et al., 2002), *mariposa* expression is eliminated rostrally but maintained in the three caudal boundaries. However, expression of *mariposa* in the hindbrain was suppressed completely by injecting *MZlzf* embryos with a *pax2* morpholino (Waskiewicz et al., 2002). Because suppression of *mariposa* expression can be caused by the simultaneous depletion of Pbx2 and Pbx4, we asked whether, in our morphants, this phenotype could be caused by *prep1.1*

knockdown-mediated reduction of Pbx proteins. However, this was not the case, because injection of *pbx4* mRNA did not rescue *mariposa* expression in *prep1.1* morphants (26 morphants observed, 21 deficient, data not shown).

Further evidence of impaired hindbrain segmentation in *prep1.1* morphants was provided by the expression of *pax2.1*.



In wild-type embryos, *pax2.1* is expressed in segmental clusters of commissural interneurons, arranged in two longitudinal rows extending from the hindbrain to the whole spinal cord (Jiang et al., 1996; Mikkola et al., 1992; Schier et al., 1996). Injection of *prep1.1*-MO caused the selective disappearance of *pax2.1*-expressing cells in the region from r2 to r6 (Fig. 4E,F), whereas injection of *pbx4*-MO did not affect the wild-type phenotype (data not shown).

We next investigated the effects of *prep1.1* knockdown on the expression of a series of markers that specify rhombomere identity. In wild-type embryos at 24 hpf, *hoxb1a* is expressed in r4, *krox20* is expressed in r3 and r5, *hoxa2* is expressed highly in r2 and r3 and at lower levels in r4 and r5, and *hoxb2* is expressed highly in r3 and r4 and at a lower level in r5 (Prince et al., 1998). Injection of *prep1.1*-MO suppressed the expression of *hoxb1a* in r4 (Fig. 4J,K). Because expression of *hoxb1a*, like that of *mariposa*, is suppressed by depletion of both Pbx2 and Pbx4 (Waskiewicz et al., 2002), we checked the effects of Pbx4 overexpression on *hoxb1a* pattern in *prep1.1* morphants. Although *hoxb1a* expression was rescued in a significant number of embryos, it always remained at minimal levels (Fig. 4T). Hence, it appears that the *hoxb1a* phenotype of the morphants was caused by the combined effects of *prep1.1* knockdown and reduced Pbx protein concentration. Nonetheless, the fact that *hoxb1a* expression was only minimally rescued by *pbx4* overexpression demonstrates that *prep1.1* is crucial for the regulation of *hoxb1a*.

In *prep1.1* morphants, *krox20* expression was abolished in r3, but not in r5 (Fig. 4Q). This effect was rescued by coinjection of *prep1.1* mRNA plus *prep1.1*-MO (Fig. 4R), which confirms the morpholino specificity. Disappearance of

Fig. 4. RNA in situ hybridization reveals disruption of hindbrain segmentation and patterning in *prep1.1* morphants. (A,B) The pattern of *hoxb1b* expression is the same as wild type (wt) in *prep1.1*-MO-treated embryos. AP indicates the animal pole, V and D indicate the ventral and dorsal side of the embryo respectively. (C,D) *prep1.1* morphants, *mariposa* expression is abolished in the six rhombomere boundaries (from r1-r2 to r6-r7). (E,F) *prep1.1* morphants lack the two rows of *pax2.1*-expressing commissural interneurons in the r2-r6 region of the hindbrain (indicated by asterisks). (G-I) The six rhombomere boundaries revealed by *pax6.1* expression (from r1-r2 to r6-r7, indicated by asterisks in the wild-type embryo) are completely lost in *prep1.1* morphants and only the r4-r5, r5-r6 and r6-r7 boundaries (asterisks) are clearly identifiable in *pbx4* morphants. (J,K) *hoxb1a* expression in r4 is lost in *prep1.1* morphants. (L-O) The levels of expression of *hoxa2* (r2-r5) and *hoxb2* (r3-r5) are severely reduced in *prep1.1* morphants. (P-S) In *prep1.1* morphants, *krox20* expression is reduced only in r3; injection of *prep1.1*-MO with a *prep1.1* mRNA construct that lacks the sequence complementary to *prep1.1*-MO rescues the wild-type phenotype. In *pbx4* morphants, *krox20* expression in r3 is also very weak. (T,U) Co-injection of *pbx4/lzr* mRNA in *prep1.1* morphants partially rescues *hoxb1a* levels but does not rescue *krox20* in r3. Embryos are stained at 60% epiboly (A,B), 20 hpf (J,K), 24 hpf (C-I,L-S). All embryos, except A and B, are in dorsal views with anterior to the left. Abbreviations: ov, otic vesicle; ncc, neural crest cells. The animals represented in this figure are different from those of Table 1. Quantitative data: (picture) probe, defective/total; (B) *hoxb1b*, 2/21; (D) *mariposa*, 21/26; (F) *pax2.1*, 25/30; (H) *pax6.1*, 16/18; (K) *hoxb1a*, 18/21; (M) *hoxa2*, 17/22; (O) *hoxb2*, 19/27; (Q) *krox20*, 19/25; (R) *krox20*, 7/20 (rescue $P < 0.01$); (S) *krox20*, 19/23; (T) *hoxb1a*, 5/11 (rescue $P < 0.05$); (U) *krox20*, 11/18.

krox20 expression in r3 was also observed in *lzf* and *MZlzf* mutants (Pöpperl et al., 2000; Waskiewicz et al., 2002) and in embryos injected with *pbx4*-MO (Fig. 4S). However, *krox20* expression in r3 was not rescued by *pbx4* mRNA overexpression in *prep1.1* morphants (Fig. 4U), indicating that *prep1.1* and *pbx4* are both crucial for expression of *krox20* in r3. By contrast, depletion of both *pbx4* and *pbx2* suppressed *krox20* expression in r3 and r5 (Waskiewicz et al., 2002). In *prep1.1*-injected embryos, expression of both *hoxa2* and *hoxb2* was reduced markedly along the whole expression domain (Fig. 4L-O), which resembles the phenotype of *lzf* mutants (Pöpperl et al., 2000). In *MZlzf* mutants, *hoxa2* expression is similarly reduced, and eliminated entirely following injection with a *pbx2* morpholino (Waskiewicz et al., 2002). Thus, the expression of *krox20* and *hoxa2* appears to be more susceptible to the elimination of the two *pbx* genes than to *prep1.1* knockdown.

***prep1.1* knockdown affects the migration of facial nerve motor neurons and causes disappearance of all reticulo-spinal neurons except Mauthner cells**

In vertebrates, the position of the motor nuclei of cranial nerves mirrors the rhombomeric organization of the hindbrain (Lumsden and Keynes, 1989). Because hindbrain segmentation and expression of rhombomere-specific genes were severely perturbed in *prep1.1* morphants, we asked whether the patterning and localization of these nuclei was also affected. We examined the expression of *islet1* (*isl1*), which is widely expressed in early postmitotic neurons (Korzh et al., 1993) and whose expression pattern in the motor nuclei of cranial nerves has been described in detail in zebrafish embryos (Chandrasekhar et al., 1997; Higashijima et al., 2000). In wild-type embryos at 48 hpf, *isl1* was detected in all motor nuclei of the hindbrain and ganglia of cranial nerves (Fig. 5A,C). In *prep1.1* morphants (Fig. 5B,D), the number of neurons that expressed *isl1* neurons in cranial nerve nuclei was not changed significantly, but their distribution was altered. In particular, the motor neurons of the facial nerve (nVII) were not located in the region that corresponded to r6 and r7 as in controls (Fig. 5A), but were spread in an elongated nucleus extending from r4-r6 (Fig. 5A-D). In zebrafish, the nVII motor neurons originate in r4 and migrate caudally to r6 and r7 (Higashijima et al., 2000). Therefore, the presence of this aggregate indicates that their migration is impaired in *prep1.1* morphants. The altered migration of nVII motor neurons to caudal regions of the hindbrain correlated well with the downregulation of *hoxb1a* in r4. In fact, knockdown of *hoxb1a* inhibits migration of nVII motor neurons (McClintock et al., 2002; Cooper et al., 2003). Further evidence of abnormal neuronal organization in the hindbrain of *prep1.1*-MO-injected embryos was revealed with antiserum to acetylated tubulin. As shown in Fig. 5K,L, neuropils and commissural tracts of the rhombomeric segments were clearly distinguishable in the controls but barely detected in *prep1.1* morphants. By contrast, the ganglion and sensory root of the trigeminal nerve (nV), were apparently unaffected by *prep1.1* inactivation, confirming the results of *isl1* expression.

RSNs are a population of individually identifiable neurons that have a rhombomere-specific localization and are sensitive to alterations in the expression of *hox* genes (Alexandre et al., 1996). A striking feature of *prep1.1* morphants at both 3 and

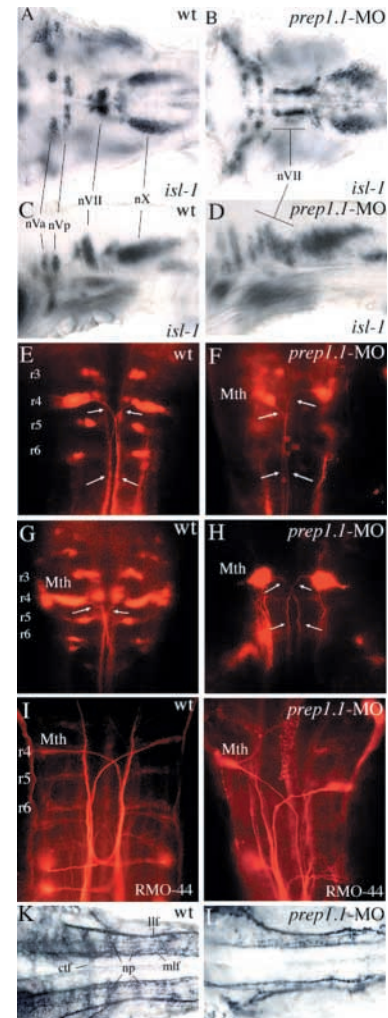
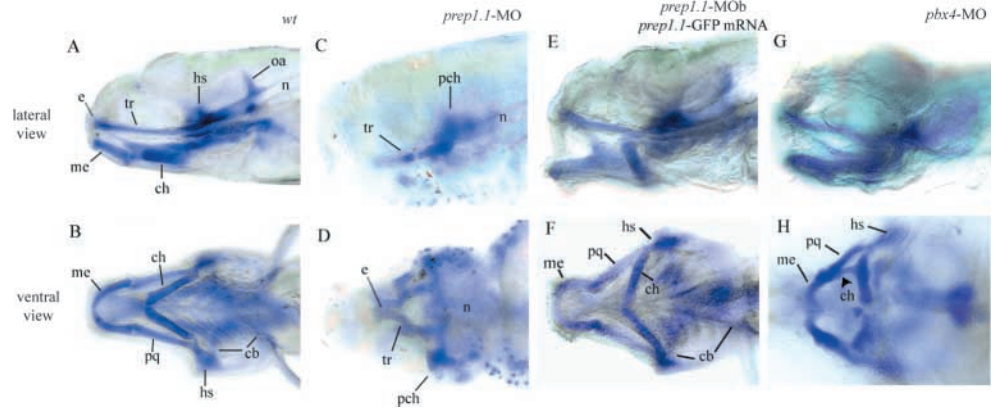


Fig. 5. Motor nuclei and ganglia of cranial nerves and reticulospinal neurons, and neuronal architecture of the hindbrain in *prep1.1* morphants. (A-D) At 48 hpf, *isl1* expression is not affected quantitatively in the motor nuclei of the cranial nerves in *prep1.1* morphants (B,D), but the motor neurons of the facial nerve (nVII) have not migrated caudally as in wild-type embryos (A,C). (E-H) Retrograde labelling with rhodamine-dextran of 3-day-old (E,F) and 5-day-old (G,H) embryos. In *prep1.1* morphants, only r4 cells are labelled; the projection of their axons (arrows) is similar to that of Mauthner cells but their morphology is slightly different. (I,J) RMO-44 antibody staining of reticulospinal neurons at 48 hpf. Only Mauthner cells are present in *prep1.1*-MO injected embryos. (K,L) At 30 hpf, the staining pattern of acetylated tubulin antiserum shows that the neuropils and commissural tract fibres, (which are mostly out of focus in wild-type embryos) are much reduced or absent in *prep1.1* morphants. Embryos are in dorsal (A,B,E-L) or lateral (C,D) views, with anterior to the left (A-D,K,L) or the top (E-L). ctf, commissural tract fibres; llf, lateral longitudinal fascicle; Mth, Mauthner cells; mlf, medial longitudinal fascicle; np, neuropil; nVa and nVp, anterior and posterior clusters of the trigeminal motor nucleus; nVII and nX, motor nuclei of the facial and vagus nerves, respectively; r, rhombomere; wt, wild-type.

5 dpf, is the disappearance of most retrogradely labelled RSNs apart from a pair of large, bilateral neurons that project contralaterally. These are identifiable as Mauthner cells that

Fig. 6. *prepl.1* morphants lack the pharyngeal skeleton. Alcian blue staining of the head skeleton of 5 day-old *prepl.1* morphants (C,D) reveals the complete lack of all pharyngeal cartilages, while those of the neurocranium are reduced. The wild-type phenotype can be substantially rescued by coinjection of *prepl.1*-MOB with a *prepl.1* mRNA construct lacking the sequence complementary to MOB (E,F). In *pbx4* morphants (G,H), the mandibular and hyoid cartilages are present, but are aberrant in shape and size and abnormally fused (arrowhead). Larvae are in lateral (A,C,E,G) and ventral (B,D,F,H) views with anterior to the left. cb, ceratobranchial; ch, ceratohyal; e, ethmoid plate; hs, hyosymplectic; me, Meckel's cartilage; n, notochord; oa, occipital arch; pch, parachordal; pq, palatoquadrate; tr, trabeculae cranii.



normally develop in r4. Given that general defects of the CNS might lead to the impossibility of backfilling RSNs, we also examined the presence and morphology of RSNs at 48 hpf using the RMO-44 antibody. The results confirmed the retrograde labelling analysis and showed that the projection of the RMO-labelled cells in *prepl.1* morphants was identical to that of Mauthner neurons in wild-type embryos (Fig. 5I,J). The results of this experiment demonstrate that Prep1.1 is necessary for the development of all RNSs except Mauthner cells.

Head cartilage defects in *prepl.1* morphants

As described above, *prepl.1* morphants lacked the jaw, indicating a defective development of neural-crest derivatives. To analyze the cranial skeletal defects induced by *prepl.1* inactivation, we examined the skull morphology using Alcian Blue staining. Five-day-old morphants lacked all neural crest-derived cartilages of the pharyngeal arches (Fig. 6C,D). The skull consisted of the neurocranium only in which the ethmoid plate and trabeculae cranii, which are thought to derive from the neural crest, were misshaped and reduced significantly in size, whereas the mesodermally-derived elements were affected much less. The phenotype induced by the *prepl.1*-MOB could be substantially rescued by co-injection of *prepl.1* (Fig. 6E,F) but not *pbx4* mRNA (data not shown). The occurrence of the cartilaginous neurocranium indicates that the lack of pharyngeal cartilages was not the consequence of a generalized block in the chondrogenic process, but the result of either patterning or specification defects. In *pbx4* morphants, the pharyngeal skeleton displayed the same defects as in *lzt* mutants (Pöpperl et al., 2000). In such embryos (Fig. 6G,H), all the branchial cartilages were missing, and the skeletal elements of the mandibular and hyoid arches were present but improperly shaped and abnormally fused.

The defects of the pharyngeal skeleton in the *prepl.1* morphants might be due to either the absence or defective migration of neural crest cells, or to their inability to differentiate into cartilage cells. To address this issue we first examined the expression of the neural crest cell marker *dlx2* (Akimenko et al., 1994). In wild-type embryos, *dlx2* is expressed in three distinct streams of cranial neural crest cells that migrate to the mandibular (m), hyoid (h) and five branchial

(b) arches (Fig. 7A). *dlx2* is also expressed in post-migratory neural crest cells within the arches (Fig. 7C). In embryos injected with *prepl.1*-MOB, *dlx2*-positive cranial neural crest cells behaved like those of wild-type embryos, gathering in three migrating streams that eventually populated the pharyngeal arches (Fig. 7B,D). The correct pattern of neural crest cell migration in *prepl.1* morphants, was further confirmed with the *snail1* marker (Fig. 7E,F), which is expressed in the head mesenchyme, in neural crest cells that give rise to the pharyngeal skeleton and in paraxial mesoderm cells that originate muscle cells (Thisse et al., 1993). The fact that *dlx2*-positive and *snail1*-positive postmigratory cells were distributed similarly in separate clusters in the pharyngeal region in both *prepl.1* morphants and wild-type embryos indicated that pharyngeal segmentation occurred normally in the morphants (Fig. 7C-F). Indeed, staining with the Zn5 antibody, confirmed that formation of the endodermal pouches and segmentation of the pharyngeal region took place correctly in *prepl.1* morphants (Fig. 7G,H).

Col2a1, which is expressed in differentiating chondrocytes, is essential for normal chondrogenesis in zebrafish and mammals (Vandenberg et al., 1991; Yan et al., 2002). Therefore, we examined whether the expression of *col2a1* was altered in postmigratory neural crest cells of *prepl.1* morphants. We found that *col2a1* was expressed in the mesenchyme that will give origin to the neurocranium in *prepl.1* morphants, though to a lesser degree than in wild-type embryos. However, it was not expressed in the pharyngeal arches (Fig. 7I-L).

Neural crest cells are known to pattern the muscles of the pharyngeal region (Noden, 1983). In zebrafish, pharyngeal chondroblasts and myoblasts differentiate synchronously, which indicates interdependence of their patterning (Schilling and Kimmel, 1994). In both *chinless* (*chn*) (Schilling et al., 1996b) and *jellyfish* (*jef*) (Yan et al., 2002) mutants, neural crest cells migrate normally to the pharyngeal region but fail to differentiate into chondrocytes. However, the pharyngeal musculature is absent in *chn* mutants but develops normally in *jef* mutants, which indicates that chondrogenesis is not a prerequisite for the differentiation of the pharyngeal musculature. To determine whether *prepl.1* knockdown affected the pharyngeal musculature we examined the

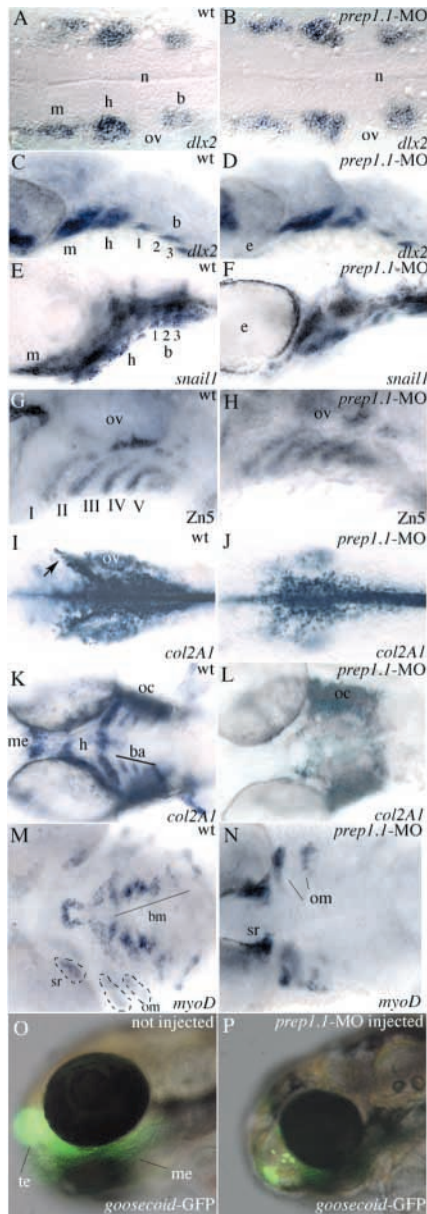


Fig. 7. Neural crest cells migrate to the pharyngeal arches in *prep1.1* morphants but do not differentiate into chondrocytes. (A,B) At 19 hpf (20-somite stage), *dlx2* expression reveals three discrete clusters of neural crest cells migrating to the mandibular (m), hyoid (h) and branchial (b) arches in wild-type embryos and *prep1.1* morphants. (C,D) At 33 hpf, in both wild-type and *prep1.1*-MO-injected embryos the *dlx2*-positive neural crest cells have reached the target position; the branchial cluster has split into three subgroups of cells. (E,F) At 48 hpf, *snail1*-expressing cells have segregated in the segmented pharyngeal arches both in wild-type embryos and *prep1.1* morphants. (G,H) At 48 hpf the pharyngeal endoderm, revealed by the Zn5 antibody, is correctly formed in *prep1.1* morphants. (I,J) At 28 hpf, *col2a1* expression in *prep1.1*-MO injected embryos reveals normal differentiation of neurocranium cartilages. However, the mesenchyme originating the parachordalia of the neurocranium is reduced (cells indicated by an arrow in I). (K,L) At 48 hpf, in the pharyngeal region of *prep1.1* morphants *col2a1* is expressed only in the otic capsule; expression is lacking in branchial arches. (M,N) At 3 dpf, in the pharyngeal region of *prep1.1* morphants *myoD* is expressed only in opercular muscles and superior rectus of the eye; expression is lacking in branchial muscles. (O,P) *prep1.1* knockdown in *gsc::GFP* transgenic larvae suppresses GFP expression in the first pharyngeal arch but not in the anterior telencephalic area. Embryos are in dorsal (A,B,I-N) and lateral (C-H,O,P) views, with anterior to the left. b, branchial arch; ba, branchial arches; bm, branchial muscles; h, hyoid arch; m, mandibular arch; me, Meckel's cartilage; n, notochord; oc, otic capsule; om, opercular muscles; ov, otic vesicle; sr, superior rectum of the eye; te, telencephalon. Quantitative data: (picture) *probe*, defective/total; (B) *dlx2*, 1/18; (D) *dlx2*, 0/22; (F) *snail1*, 4/25; (H) *zn5*, 4/18; (J) *col2a1*, 18/21; (L) *col2a1*, 18/19; (N) *myoD*, 16/18; (P) *gsc*, 4/5.

gsc promoter, which express GFP in the embryonal brain and mandibular cartilage (Doitsidou et al., 2002). Knockdown of *prep1.1* in transgenic larvae suppressed GFP expression in the first pharyngeal arch but not in the anterior telencephalic area (Fig. 7O,P). This result shows that Prep1.1 activity is required for the expression of *gsc* in the mandibular arch, which indicates that *prep1.1* is necessary for both arch patterning and pharyngeal chondrogenesis.

Hence, in *prep1.1* morphants, cranial neural crest cells were present and migrated correctly to the pharyngeal region, which was properly segmented by the endodermal pouches but failed to undergo chondrogenesis. In addition, the muscles connected to the pharyngeal cartilages did not develop.

expression of *myoD*, the early marker of myogenesis, in *prep1.1* morphants. At a stage in which all head muscles of wild-type larvae express *myoD*, expression of *myoD* in the head of the morphants was detected in the eye muscles and in few lateral elements, seemingly opercular muscles, but not in the pharyngeal region (Fig. 7M,N).

In zebrafish, there are two independent phases of expression of the homeobox gene *gooseoid* (*gsc*), a gene that is required for cranio-facial development in mammals (Clouthier et al., 2000; Zhu et al., 1997): an early phase in cells anterior to the presumptive notochord; and a late phase at 2-3 dpf in the brain and in neural crest derivatives of the mandibular and hyoid arches (Schulte-Merker et al., 1994). In zebrafish, expression of *gsc* in mandibular and hyoid arches is dependant on Hoxa2 function (Hunter and Prince, 2002). To assess whether *gsc* expression was affected by *prep1.1* knockdown we used transgenic zebrafish that contain a GFP construct driven by a

Discussion

In the present work we describe the effects of the morpholino-induced inactivation of the *prep1.1* gene in zebrafish embryos. Four major features are characteristic of *prep1.1* morphants: (1) prominent apoptotic cell death, which becomes evident at the 15-somite stage in the neuroectoderm and peaks at 24-36 hpf in the CNS, particularly in the hindbrain; (2) loss of expression of several genes, in particular *hox* members, in specific rhombomeres; (3) defective hindbrain patterning; and (4) lack of all neural crest-derived cartilages in the head skeleton. Moreover, using a *pbx4*-MO, that reproduced faithfully the *lzx* phenotype, we provide evidence that Prep1.1 and Pbx4 interact in certain developmental processes but act independently in others.

The maternal expression of *prep1.1* and its ubiquitous distribution in zebrafish embryos up to 24 hpf indicated

its involvement in early embryogenetic processes. This assumption was confirmed by our finding that inactivation of *prep1.1* induced prominent apoptosis, which becomes clearly visible during somitogenesis. Accordingly, the time course of the nuclear translocation of Prep1.1-GFP, demonstrated that the mechanisms required for the nuclear import of Prep1.1, which is a prerequisite for its activity, are fully functional by the end of gastrulation. Like other Meinox proteins, Prep1.1 lacks a nuclear-localization signal and relies on Pbc partners for translocation to the nucleus (Berthelsen et al., 1999). Because Pbx4 and Pbx2 are the main Pbc members that are expressed early in zebrafish embryogenesis (Pöpperl et al., 2000; Waskiewicz et al., 2002), they appear to be the major Prep1.1 partners in early zebrafish development. Indeed, this is supported by the observation that Prep1.1-GFP remains mostly cytoplasmic in both *pbx4* and *pbx2/pbx4* double morphants. However, in such morphants, the finding that some Prep1.1-GFP was associated with the nucleus, is consistent with the occurrence of maternal Pbx4 in early developmental stages (Waskiewicz et al., 2002).

As evidenced by immunoblotting analysis, Prep1.1 affects the levels of Pbx2 and Pbx4 and, possibly, of other Pbx members. The effect is probably post-transcriptional and might be caused by a longer half-life of Pbx proteins when they form dimers with either Prep and Meis. In fact, in *Drosophila*, Exd is destabilized and degraded in the absence of Hth (Kurant et al., 2001), and lack of Prep1 in mice coincides with a strong, widespread reduction of the levels of all Pbx proteins (E.F. and F.B., unpublished). Moreover, overexpression of Prep1 in mouse teratocarcinoma cells increases the half-life and, therefore, the level of Pbx proteins (Longobardi and Blasi, 2003). As simultaneous depletion of Pbx2 and Pbx4 also causes a series of molecular and morphological effects that are similar to the phenotypes observed in *prep1.1* morphants (Waskiewicz et al., 2002), such a phenotype might be due to the reverberating effects of Prep1.1 suppression on the levels of Pbx proteins. However, this was apparently not the case. In fact, the inability of *pbx4/lzr* mRNA to rescue apoptosis, expression of *mariposa* in rhombomere boundaries, expression of *krox20* in r3 and branchial cartilage formation in *prep1.1* morphants, reveals a direct role of *prep1.1* in embryo development other than the mere stabilization of Pbx proteins.

Suppression of *prep1.1* induces apoptosis

Meinox proteins control differentiation through a wide array of interactions with different homeodomain transcription factors. Thus, the apoptotic process observed in *prep1.1* morphants might be caused by the programmed cell death of cells that fail to differentiate (Ishizaki et al., 1995). It is noteworthy that the morphological phenotype of *prep1.1* morphants shares similarities with the *spacehead* class (group II) of zebrafish mutants described by Abdelilah et al. (Abdelilah et al., 1996). In particular, the onset of apoptosis coincides temporally and spatially in *prep1.1* morphants and *spacehead* mutants. Interestingly, it was proposed that the genes affected in *spacehead* mutants are involved in either the differentiation or maintenance of neural cell types, suggesting that cells that are unable to conclude their differentiation process are fated to death by apoptosis (Abdelilah et al., 1996). Links between Meinox partners such as mouse Hoxa1 and Hoxb1 (which are the orthologous of zebrafish Hoxb1b and

Hoxb1a, respectively) and apoptosis have been established recently (Barrow et al., 2000; Lohmann et al., 2002). Thus, the prominent apoptotic process observed in *prep1.1* morphants might be related to an impaired activity of Hox proteins due to *prep1.1* inactivation.

Suppression of *prep1.1* affects the expression of genes crucial for hindbrain development

Our results show that *prep1.1* morphants exhibit major changes of gene expression patterns in the hindbrain. First, although expression of *hoxb1b*, the orthologue of mouse *Hoxa1*, is not affected, *hoxb1a*, the orthologue of mouse *Hoxb1*, which is normally expressed in r4, is absent. Moreover, we show that the expression of *hoxa2* and *hoxb2* is strongly reduced. Meinox proteins form functionally active heterotrimeric complexes with Pbx and Hox and these complexes are functionally important *in vivo* in the expression of at least *Hoxb2* in r4 and r6-r8 (Jacobs et al., 1999; Ryoo et al., 1999; Ferretti et al., 2000). However, the Meinox protein involved has not been identified. In zebrafish, *hoxb1a* expression in r4 requires *pbx2/4* and *hoxb1b* (Cooper et al., 2003; Waskiewicz et al., 2001; Waskiewicz et al., 2002). Because *prep1.1* is required for full expression of *hoxb1a* in r4, the expression of this gene might also require the formation of a heterotrimeric complex between *prep1.1*, *pbx2/4* and *hoxb1b* gene products. Although the role of heterotrimeric complexes was not apparent in initial investigations of *Hoxb1* expression (Jacobs et al., 1999; Ferretti et al., 2000), we have observed that, in mice, the r4 *Hoxb1* enhancer extends slightly more 3' than previously defined, and heterotrimeric Meinox-Pbc-Hox complexes might be required for *Hoxb1* expression (E. Ferretti, R. Krumlauf and F. Blasi, in preparation).

In the mouse, expression of *Hoxb2* depends on *krox20* in r3 and r5, and on the heterotrimeric Meinox-Pbx-Hox complex in r4 (Jacobs et al., 1999; Ryoo et al., 1999; Ferretti et al., 2001). Here, we show that *hoxb2* expression requires *prep1.1* in r2, r4 and r3. The effect observed in r3 is probably due to the absence of *krox20*, whereas in r4 it might depend directly on the lack of *prep1.1* as well as the induced decrease of *pbx4*. In conclusion, because the absence of *prep1.1* results in the absence of *hoxb1a*, *prep1.1* inactivation causes the decrease/absence of all factors that are required for activity of the *hoxb2* enhancer *Krox20* in r3 and the heterotrimeric complex in r4. The lack of expression of *krox20* in *prep1.1* morphants is also reflected by the absence of *hoxa2* expression in r3. Conversely, in *prep1.1* morphants *krox20* is expressed normally in r5, in which *hoxa2* and *hoxb2* are absent. These results show unique properties of the Prep1.1 protein in the specification of r2-r5.

prep1.1 is crucial for hindbrain patterning

The vertebrate hindbrain exerts a key function in patterning the developing head through its segmental rhombomeric structure and its ability to generate neural crest cells. Rhombomeres direct the proper organization of cranial ganglia, branchiomotor nerves and the migration of neural crest cells (Trainor and Krumlauf, 2000). Our results show that Prep1.1 is crucial for hindbrain segmentation. This is illustrated in *prep1.1* morphants by the loss of the segmental expression patterns of *mariposa* and *pax6.1* throughout the hindbrain, and the absence of *pax2.1*-positive commissural interneurons in the

r2-r6 region. Unlike Prep1.1, Pbx4 is necessary for hindbrain segmentation only anteriorly to the r4-r5 boundary. In fact, in our *pbx4* morphants, and in embryos expressing a dominant negative derivative of *pbx4* (Choe et al., 2002), *pax6.1* segmentation is lost anteriorly but not posteriorly to the r4-r5 boundary. This is in accord with the loss of rhombomere segmentation anterior to the r4-r5 boundary in *lzf* mutants revealed by *mariposa* expression (Pöpperl et al., 2000).

On the basis of the effects of *prep1.1*, *pbx4* and *pbx2* inactivation on hindbrain patterning (Fig. 4) (Waskiewicz et al., 2002), and of the deficiencies in *hox* gene expression in the hindbrain (Fig. 4), it can be deduced that Prep1.1 regulates the process of rhombomeric segmentation and specification by acting with Pbx4 rostral to the r4-r5 boundary, and with Pbx4 and Pbx2 caudal to that boundary.

Another striking effect of *prep1.1* inactivation on hindbrain development is the lack of RSNs except Mauthner cells. This feature indicates that Prep1.1 is necessary for early differentiation and/or survival of most RSNs. By contrast, *pbx4* would be required subsequently for the acquisition of the identity of RSNs, as shown in *lzf* mutants in which all RSNs located posteriorly to r2 display r2 identity (Pöpperl et al., 2000). Although r4 identity is disrupted in *prep1.1* morphants, as evidenced by the absence of *hoxb1a* expression, the occurrence of r4-specific Mauthner cells is not incongruous. In fact, Mauthner cells appear normally at 7.5 hpf, so their differentiation is independent of *hoxb1a*, whose expression starts ~2 hours later (Prince et al., 1998; McClintock et al., 2001). Indeed, the development of Mauthner cells requires *hoxb1b*, which is expressed first at 6 hpf in the presumptive r4 (Alexandre et al., 1996; McClintock et al., 2001) and is normally expressed in *prep1.1* morphants. Being independent of *prep1.1*, the development of Mauthner cells might require another Meinox member. This possibility is indicated by the disappearance of Mauthner neurons in embryos that express a dominant negative derivative of Pbx4 (Choe et al., 2002), and is supported by the high level of expression of other Meinox genes in r4 during somitogenesis (Waskiewicz et al., 2001).

***prep1.1* is indispensable for the development of the pharyngeal skeleton**

The selective lack of all neural crest-derived cartilages of the head skeleton and pharyngeal muscles are major traits shared by *prep1.1* morphants and *chn* mutants (Schilling et al., 1996b). It is noteworthy that none of the 109 (Piotrowski et al., 1996; Schilling et al., 1996a) and 48 (Neuhauss et al., 1996) mutants with cranio-facial abnormalities that were obtained in large-scale screens for mutations that affect early zebrafish development lacked specifically all the cartilages derived from the neural crest. Thus *prep1.1* is the only gene so far identified that is indispensable for the development of the whole pharyngeal skeleton and it might be involved in a common genetic pathway with *chn*. In *prep1.1* morphants, as in *chn* mutants (Schilling et al., 1996b), the particular phenotype is caused neither by a general defect in the process of chondrogenesis because the mesodermally derived cartilages of the neurocranium are present, nor to the lack and unsuccessful migration of neural crest cells into the pharyngeal arches, as evidenced by *dlx2* and *snail1* labelling (Fig. 7). Hence, it appears that cartilage precursors of the pharyngeal arches lack the capacity to differentiate into chondrocytes in the absence of

prep1.1. It has been shown that segmentation of the pharyngeal endoderm is required for the correct patterning of the cartilages of the pharyngeal arches. Indeed, in *lzf* mutants, in which endodermal pouches do not form, only deformed and fused mandibular and hyoid cartilages develop (Pöpperl et al., 2000). Moreover, in *van gogh* (*vgo*) mutants, in which only the first endodermal pouch develops, the cartilages of the mandibular and hyoid arches do occur, whereas those of the posterior (P3-P7) arches are highly reduced (Piotrowski and Nüsslein-Volhard, 2000). However, in *prep1.1* morphants, the pharyngeal region is segmented normally and the pharyngeal endoderm is patterned correctly. Hence, our results indicate that in *prep1.1* morphants the absence of all pharyngeal cartilages is caused either by a primary specification defect of neural crest cells or by the lack of competence/signals necessary for chondrogenic differentiation of specified cells. The fact that in *lzf* and *vgo* mutants pharyngeal cartilaginous structures do occur, albeit heavily reduced and improperly shaped, indicates that endodermal segmentation is not indispensable for chondrogenesis, although it affects profoundly its patterning. Hence, the very process of differentiation of neural crest cells into chondrocytes within the pharyngeal arches appears to be independent of endodermal segmentation. The complete lack of P3-P7 cartilages in *lzf* mutants and *pbx4* morphants might, thus, be explained by the failure of a process that requires the Prep1.1-Pbx4 partnership. If this hypothesis is correct, chondrogenesis in P1 and P2 would require Prep1.1 and a Pbc partner other than Pbx4, consistent with the occurrence of mandibular and hyoid cartilages in *lzf* mutants. Thus, pharyngeal endodermal segmentation would need Pbx4, whereas chondrocyte differentiation in all pharyngeal arches would require Prep1.1 in association with Pbx4 in P3-P7 and another Pbc partner, possibly Pbx2, in P1 and P2. Indeed, the homeotic transformation of the cartilages of the hyoid arch into those of the mandibular arch in *lzf* mutants (Pöpperl et al., 2000), confirms that Pbx4 is required for P2 cartilage identity but not for its histogenesis. Finally, the defective hindbrain segmentation in the presence of a normally segmented pharyngeal endoderm in *prep1.1* morphants, supports the hypothesis (Piotrowski and Nüsslein-Volhard, 2000) that the two processes are independent and based on different molecular mechanisms.

Our data show that Prep1.1 is uniquely involved in essential aspects of embryo development, in particular hindbrain patterning, cell differentiation and apoptosis. Some effects might be ascribed to the interaction with either Pbx4 or Pbx2 and appear to be dependent on transcriptional effects on Hox genes. The presence of at least two Prep and three Meis proteins in zebrafish embryos (Waskiewicz et al., 2001), and the fact that the Prep proteins are expressed ubiquitously in early development, might indicate redundant functions. Indeed, *in vitro* experiments have failed to show differences in the ability of different Meinox proteins to interact with Pbx or to produce ternary complexes with Hox members. However, the results of *prep1.1* inactivation demonstrate some specificity, indicating the occurrence of mechanisms based on different specific combinations of Meinox and Pbc proteins. The functional inactivation of *prep1.1* in zebrafish is the first attempt to dissect the function of the various Meinox proteins in development. Further work will undoubtedly highlight the role of the other Meinox proteins.

This work was supported by MURST (Italian Ministry of University and Scientific Research) and Telethon. We wish to thank Stefano Piccolo, Bernard Peers and Cecilia Moens for critical reading of the manuscript. We are indebted to Stefano di Narda and Suscha Greguoldo for their contributions, and all members of the Zebrafish Laboratory in Padua for helpful suggestions. We are indebted to Heike Pöpperl for the generous gift of Pan-Pbx antibodies, Cecilia Moens for the *pbx2* morpholino and Bernard Peers for the *prep1.1*-MOa. GD and NT are supported by research fellowships funded by MURST and EU respectively.

References

- Abdelilah, S., Mountcastle-Shah, E., Harvey, M., Solnica-Krezel, L., Schier, A. F., Stemple, D. L., Malicki, J., Neuhauss, S. C., Zwartkruis, F., Stainier, D. Y. et al. (1996). Mutations affecting neural survival in the zebrafish *Danio rerio*. *Development* **123**, 217-227.
- Abrams, J. M. (1999). An emerging blueprint for apoptosis in *Drosophila*. *Trends Cell Biol.* **9**, 435-440.
- Abu-Shaar, M., Ryoo, H. D. and Mann, R. S. (1999). Control of the nuclear localization of Extradenticle by competing nuclear import and export signals. *Genes Dev.* **13**, 935-945.
- Akimenko, M. A., Ekker, M., Wegner, J., Lin, W. and Westerfield, M. (1994). Combinatorial expression of three zebrafish genes related to distal-less: part of a homeobox gene code for the head. *J. Neurosci.* **14**, 3475-3486.
- Alexandre, D., Clarke, J. D., Oxtoby, E., Yan, Y. L., Jowett, T. and Holder, N. (1996). Ectopic expression of Hoxa-1 in the zebrafish alters the fate of the mandibular arch neural crest and phenocopies a retinoic acid-induced phenotype. *Development* **122**, 735-746.
- Barrow, J. R., Stadler, H. S. and Capecchi, M. R. (2000). Roles of Hoxa1 and Hoxa2 in patterning the early hindbrain of the mouse. *Development* **127**, 933-944.
- Berthelsen, J., Viggiano, L., Schulz, H., Ferretti, E., Consalez, G. G., Rocchi, M. and Blasi, F. (1998a). PKNOX1, a gene encoding PREP1, a new regulator of Pbx activity, maps on human chromosome 21q22.3 and murine chromosome 17B/C. *Genomics* **47**, 323-324.
- Berthelsen, J., Zappavigna, V., Ferretti, E., Mavilio, F. and Blasi, F. (1998b). The novel homeoprotein Prep1 modulates Pbx-Hox protein cooperativity. *EMBO J.* **17**, 1434-1445.
- Berthelsen, J., Kilstrup-Nielsen, C., Blasi, F., Mavilio, F. and Zappavigna, V. (1999). The subcellular localization of PBX1 and EXD proteins depends on nuclear import and export signals and is modulated by association with PREP1 and HTH. *Genes Dev* **13**, 946-953.
- Biemar, F., Devos, N., Martial, J. A., Driever, W. and Peers, B. (2001). Cloning and expression of the TALE superclass homeobox Meis2 gene during zebrafish embryonic development. *Mech. Dev.* **109**, 427-431.
- Burglin, T. R. (1997). Analysis of TALE superclass homeobox genes (MEIS, PBC, KNOX, Iroquois, TGIF) reveals a novel domain conserved between plants and animals. *Nucleic Acids Res.* **25**, 4173-4180.
- Capdevila, J. and Belmonte, J. C. (1999). Extracellular modulation of the Hedgehog, Wnt and TGF-beta signalling pathways during embryonic development. *Curr. Opin. Genet. Dev.* **9**, 427-433.
- Chandrasekhar, A., Moens, C. B., Warren, J. T., Jr, Kimmel, C. B. and Kuwada, J. Y. (1997). Development of branchiomotor neurons in zebrafish. *Development* **124**, 2633-2644.
- Choe, S. K., Vlachakis, N. and Sagerstrom, C. G. (2002). Meis family proteins are required for hindbrain development in the zebrafish. *Development* **129**, 585-595.
- Clothier, D. E., Williams, S. C., Yanagisawa, H., Wieduwilt, M., Richardson, J. A. and Yanagisawa, M. (2000). Signaling pathways crucial for craniofacial development revealed by endothelin-A receptor-deficient mice. *Dev. Biol.* **217**, 10-24.
- Cooper, K. L., Leisenring, W. M. and Moens, C. B. (2003). Autonomous and nonautonomous functions for Hox/Pbx in branchiomotor neuron development. *Dev. Biol.* **253**, 200-213.
- Dibner, C., Elias, S. and Frank, D. (2001). XMeis3 protein activity is required for proper hindbrain patterning in *Xenopus laevis* embryos. *Development* **128**, 3415-3426.
- Doitsidou, M., Reichman-Fried, M., Stebler, J., Kopranner, M., Dorries, J., Meyer, D., Eguerra, C. V., Leung, T. and Raz, E. (2002). Guidance of primordial germ cell migration by the chemokine SDF-1. *Cell* **111**, 647-659.
- Ferretti, E., Marshall, H., Pöpperl, H., Maconochie, M., Krumlauf, R. and Blasi, F. (2000). Segmental expression of *Hoxb2* in r4 requires two separate sites that integrate cooperative interactions between Prep1, Pbx and Hox proteins. *Development* **127**, 155-166.
- Fognani, C., Kilstrup-Nielsen, C., Berthelsen, J., Ferretti, E., Zappavigna, V. and Blasi, F. (2002). Characterization of PREP2, a paralog of PREP1, which defines a novel sub-family of the MEINOX TALE homeodomain transcription factors. *Nucleic Acids Res.* **30**, 2043-2051.
- Haller, K., Rambaldi, I., Kovacs, E. N., Daniels, E. and Featherstone, M. (2002). Prep2: cloning and expression of a new prep family member. *Dev. Dyn.* **225**, 358-364.
- Higashijima, S., Hotta, Y. and Okamoto, H. (2000). Visualization of cranial motor neurons in live transgenic zebrafish expressing green fluorescent protein under the control of the *islet-1* promoter/enhancer. *J. Neurosci.* **20**, 206-218.
- Hunter, M. P. and Prince, V. E. (2002). Zebrafish hox paralogue group 2 genes function redundantly as selector genes to pattern the second pharyngeal arch. *Dev. Biol.* **247**, 367-389.
- Ishizaki, Y., Cheng, L., Mudge, A. W. and Raff, M. C. (1995). Programmed cell death by default in embryonic cells, fibroblasts, and cancer cells. *Mol. Biol. Cell* **6**, 1443-1458.
- Jacobs, Y., Schnabel, C. A. and Cleary, M. L. (1999). Trimeric association of Hox and TALE homeodomain proteins mediates Hoxb2 hindbrain enhancer activity. *Mol. Cell Biol.* **19**, 5134-5142.
- Jiang, Y. J., Brand, M., Heisenberg, C. P., Beuchle, D., Furutani-Seiki, M., Kelsh, R. N., Warga, R. M., Granato, M., Haffter, P., Hammerschmidt, M. et al. (1996). Mutations affecting neurogenesis and brain morphology in the zebrafish, *Danio rerio*. *Development* **123**, 205-216.
- Kamps, M. P., Murre, C., Sun, X. H. and Baltimore, D. (1990). A new homeobox gene contributes the DNA binding domain of the t(1;19) translocation protein in pre-B ALL. *Cell* **60**, 547-555.
- Korzh, V., Edlund, T. and Thor, S. (1993). Zebrafish primary neurons initiate expression of the LIM homeodomain protein Isl-1 at the end of gastrulation. *Development* **118**, 417-425.
- Krauss, S., Johansen, T., Korzh, V. and Fjose, A. (1991). Expression of the zebrafish paired box gene pax[zf-b] during early neurogenesis. *Development* **113**, 1193-1206.
- Krumlauf, R. (1994). Hox genes in vertebrate development. *Cell* **78**, 191-201.
- Kurant, E., Eytan, D. and Salzberg, A. (2001). Mutational analysis of the *Drosophila* homothorax gene. *Genetics* **157**, 689-698.
- Lohmann, I., McGinnis, N., Bodmer, M. and McGinnis, W. (2002). The *Drosophila* Hox gene deformed sculpts head morphology via direct regulation of the apoptosis activator reaper. *Cell* **110**, 457-466.
- Longobardi, E. and Blasi, F. (2003). Overexpression of PREP-1 leads to a functionally relevant increase of PBX-2 by preventing its degradation. *J. Biol. Chem.* Jul 2003; 10.1074/jbc.M304704200 (October 2003).
- Lumsden, A. and Keynes, R. (1989). Segmental patterns of neuronal development in the chick hindbrain. *Nature* **337**, 424-428.
- Mann, R. S. and Chan, S. K. (1996). Extra specificity from extradenticle: the partnership between HOX and PBX/EXD homeodomain proteins. *Trends Genet.* **12**, 258-262.
- McClintock, J. M., Carlson, R., Mann, D. M. and Prince, V. E. (2001). Consequences of Hox gene duplication in the vertebrates: an investigation of the zebrafish Hox paralogue group 1 genes. *Development* **128**, 2471-2484.
- McClintock, J. M., Kheirbek, M. A. and Prince, V. E. (2002). Knockdown of duplicated zebrafish hoxb1 genes reveals distinct roles of hindbrain patterning and a novel mechanism of duplicate gene retention. *Development* **129**, 2339-2354.
- Mercader, N., Leonardo, E., Azpiazu, N., Serrano, A., Morata, G., Martinez, C. and Torres, M. (1999). Conserved regulation of proximal-distal limb axis development by Meis1/Hth. *Nature* **402**, 425-429.
- Mikkola, I., Fjose, A., Kuwada, J. Y., Wilson, S., Guddal, P. H. and Krauss, S. (1992). The paired domain-containing nuclear factor pax[b] is expressed in specific commissural interneurons in zebrafish embryos. *J. Neurobiol.* **23**, 933-946.
- Moens, C. B. and Prince, V. E. (2002). Constructing the hindbrain: insights from the zebrafish. *Dev. Dyn.* **224**, 1-17.
- Moens, C. B., Yan, Y. L., Appel, B., Force, A. G. and Kimmel, C. B. (1996). valentino: a zebrafish gene required for normal hindbrain segmentation. *Development* **122**, 3981-3990.
- Nasevicius, A. and Ekker, S. C. (2000). Effective targeted gene 'knockdown' in zebrafish. *Nat. Genet.* **26**, 216-220.
- Neuhauss, S. C., Solnica-Krezel, L., Schier, A. F., Zwartkruis, F., Stemple, D. L., Malicki, J., Abdelilah, S., Stainier, D. Y. and Driever, W. (1996).

- Mutations affecting craniofacial development in zebrafish. *Development* **123**, 357-367.
- Noden, D. M.** (1983). The role of the neural crest in patterning of avian cranial skeletal, connective, and muscle tissues. *Dev. Biol.* **96**, 144-165.
- Nourse, J., Mellentin, J. D., Galili, N., Wilkinson, J., Stanbridge, E., Smith, S. D. and Cleary, M. L.** (1990). Chromosomal translocation t(1;19) results in synthesis of a homeobox fusion mRNA that codes for a potential chimeric transcription factor. *Cell* **60**, 535-545.
- Oxtoby, E. and Jowett, T.** (1993). Cloning of the zebrafish *krox-20* gene (*krx-20*) and its expression during hindbrain development. *Nucleic Acids Res.* **21**, 1087-1095.
- Piotrowski, T. and Nüsslein-Volhard, C.** (2000). The endoderm plays an important role in patterning the segmented pharyngeal region in zebrafish (*Danio rerio*). *Dev. Biol.* **225**, 339-356.
- Piotrowski, T., Schilling, T. F., Brand, M., Jiang, Y. J., Heisenberg, C. P., Beuchle, D., Grandel, H., van Eeden, F. J., Furutani-Seiki, M., Granato, M. et al.** (1996). Jaw and branchial arch mutants in zebrafish II: anterior arches and cartilage differentiation. *Development* **123**, 345-356.
- Pöpperl, H., Rikhof, H., Chang, H., Haffter, P., Kimmel, C. B. and Moens, C. B.** (2000). lazarus is a novel pbx gene that globally mediates hox gene function in zebrafish. *Mol Cell* **6**, 255-267.
- Prince, V. E., Moens, C. B., Kimmel, C. B. and Ho, R. K.** (1998). Zebrafish hox genes: expression in the hindbrain region of wild-type and mutants of the segmentation gene, valentino. *Development* **125**, 393-406.
- Puschel, A. W., Westerfield, M. and Dressler, G. R.** (1992). Comparative analysis of Pax-2 protein distributions during neurulation in mice and zebrafish. *Mech. Dev.* **38**, 197-208.
- Ryoo, H. D., Marty, T., Casares, F., Affolter, M. and Mann, R. S.** (1999). Regulation of Hox target genes by a DNA bound Homothorax/Hox/Extradenticle complex. *Development* **126**, 5137-5148.
- Sachdev, S. W., Dietz, U. H., Oshima, Y., Lang, M. R., Knapik, E. W., Hiraki, Y. and Shukunami, C.** (2001). Sequence analysis of zebrafish chondromodulin-1 and expression profile in the notochord and chondrogenic regions during cartilage morphogenesis. *Mech. Dev.* **105**, 157-162.
- Salzberg, A., Elias, S., Nachaliel, N., Bonstein, L., Henig, C. and Frank, D.** (1999). A Meis family protein caudalizes neural cell fates in *Xenopus*. *Mech. Dev.* **80**, 3-13.
- Schier, A. F., Neuhauss, S. C., Harvey, M., Malicki, J., Solnica-Krezel, L., Stainier, D. Y., Zwartkruis, F., Abdelilah, S., Stemple, D. L., Rangini, Z. et al.** (1996). Mutations affecting the development of the embryonic zebrafish brain. *Development* **123**, 165-178.
- Schilling, T. F. and Kimmel, C. B.** (1994). Segment and cell type lineage restrictions during pharyngeal arch development in the zebrafish embryo. *Development* **120**, 483-494.
- Schilling, T. F., Piotrowski, T., Grandel, H., Brand, M., Heisenberg, C. P., Jiang, Y. J., Beuchle, D., Hammerschmidt, M., Kane, D. A., Mullins, M. C. et al.** (1996a). Jaw and branchial arch mutants in zebrafish I: branchial arches. *Development* **123**, 329-344.
- Schilling, T. F., Walker, C. and Kimmel, C. B.** (1996b). The chinless mutation and neural crest cell interactions in zebrafish jaw development. *Development* **122**, 1417-1426.
- Schulte-Merker, S., Hammerschmidt, M., Beuchle, D., Cho, K. W., De Robertis, E. M. and Nüsslein-Volhard, C.** (1994). Expression of zebrafish gooseoid and no tail gene products in wild-type and mutant no tail embryos. *Development* **120**, 843-852.
- Selleri, L., Depew, M. J., Jacobs, Y., Chanda, S. K., Tsang, K. Y., Cheah, K. S., Rubenstein, J. L., O'Gorman, S. and Cleary, M. L.** (2001). Requirement for Pbx1 in skeletal patterning and programming chondrocyte proliferation and differentiation. *Development* **128**, 3543-3557.
- Shen, W. F., Montgomery, J. C., Rozenfeld, S., Moskow, J. J., Lawrence, H. J., Buchberg, A. M. and Largman, C.** (1997). AbdB-like Hox proteins stabilize DNA binding by the Meis1 homeodomain proteins. *Mol. Cell. Biol.* **17**, 6448-6458.
- Thisse, C., Thisse, B., Schilling, T. F. and Postlethwait, J. H.** (1993). Structure of the zebrafish *snail1* gene and its expression in wild-type, spadetail and no tail mutant embryos. *Development* **119**, 1203-2115.
- Thorsteinsdottir, U., Kroon, E., Jerome, L., Blasi, F. and Sauvageau, G.** (2001). Defining roles for HOX and MEIS1 genes in induction of acute myeloid leukemia. *Mol. Cell. Biol.* **21**, 224-234.
- Trainor, P. A. and Krumlauf, R.** (2000). Patterning the cranial neural crest: hindbrain segmentation and Hox gene plasticity. *Nat. Rev. Neurosci.* **1**, 116-124.
- Van Auken, K., Weaver, D., Robertson, B., Sundaram, M., Saldi, T., Edgar, L., Elling, U., Lee, M., Boese, Q. and Wood, W. B.** (2002). Roles of the Homothorax/Meis/Prep homolog UNC-62 and the Exd/Pbx homologs CEH-20 and CEH-40 in *C. elegans* embryogenesis. *Development* **129**, 5255-5268.
- Vandenberg, P., Khillan, J. S., Prockop, D. J., Helminen, H., Kontusaari, S. and Ala-Kokko, L.** (1991). Expression of a partially deleted gene of human type II procollagen (COL2A1) in transgenic mice produces a chondrodysplasia. *Proc. Natl. Acad. Sci. USA* **88**, 7640-7644.
- Vlachakis, N., Choe, S. K. and Sagerstrom, C. G.** (2001). Meis3 synergizes with Pbx4 and Hoxb1b in promoting hindbrain fates in the zebrafish. *Development* **128**, 1299-1312.
- Wagner, K., Mincheva, A., Korn, B., Lichter, P. and Pöpperl, H.** (2001). Pbx4, a new Pbx family member on mouse chromosome 8, is expressed during spermatogenesis. *Mech. Dev.* **103**, 127-131.
- Waskiewicz, A. J., Rikhof, H. A., Hernandez, R. E. and Moens, C. B.** (2001). Zebrafish Meis functions to stabilize Pbx proteins and regulate hindbrain patterning. *Development* **128**, 4139-4151.
- Waskiewicz, A. J., Rikhof, H. A. and Moens, C. B.** (2002). Eliminating zebrafish pbx proteins reveals a hindbrain ground state. *Dev. Cell* **3**, 723-733.
- Weinberg, E. S., Allende, M. L., Kelly, C. S., Abdelhamid, A., Murakami, T., Andermann, P., Doerre, O. G., Grunwald, D. J. and Riggleman, B.** (1996). Developmental regulation of zebrafish MyoD in wild-type, no tail and spadetail embryos. *Development* **122**, 271-280.
- Williams, J. A., Barrios, A., Gatchalian, C., Rubin, L., Wilson, S. W. and Holder, N.** (2000). Programmed cell death in zebrafish rohn beard neurons is influenced by TrkC1/NT-3 signaling. *Dev. Biol.* **226**, 220-230.
- Yan, Y. L., Miller, C. T., Nissen, R. M., Singer, A., Liu, D., Kirn, A., Draper, B., Willoughby, J., Morcos, P. A., Amsterdam, A. et al.** (2002). A zebrafish *sox9* gene required for cartilage morphogenesis. *Development* **129**, 5065-5079.
- Zhu, C. C., Yamada, G. and Blum, M.** (1997). Correlation between loss of middle ear bones and altered gooseoid gene expression in the branchial region following retinoic acid treatment of mouse embryos *in vivo*. *Biochem. Biophys. Res. Commun.* **235**, 748-753.